



Submitted to: JHEP



CERN-PH-EP-2015-320
18th March 2016

Search for new phenomena with photon+jet events in proton–proton collisions at $\sqrt{s} = 13$ TeV with the ATLAS detector

The ATLAS Collaboration

Abstract

A search is performed for the production of high-mass resonances decaying into a photon and a jet in 3.2 fb^{-1} of proton–proton collisions at a centre-of-mass energy of $\sqrt{s} = 13$ TeV collected by the ATLAS detector at the Large Hadron Collider. Selected events have an isolated photon and a jet, each with transverse momentum above 150 GeV. No significant deviation of the γ +jet invariant mass distribution from the background-only hypothesis is found. Limits are set at 95% confidence level on the cross sections of generic Gaussian-shaped signals and of a few benchmark phenomena beyond the Standard Model: excited quarks with vector-like couplings to the Standard Model particles, and non-thermal quantum black holes in two models of extra spatial dimensions. The minimum excluded visible cross sections for Gaussian-shaped resonances with width-to-mass ratios of 2% decrease from about 6 fb for a mass of 1.5 TeV to about 0.8 fb for a mass of 5 TeV. The minimum excluded visible cross sections for Gaussian-shaped resonances with width-to-mass ratios of 15% decrease from about 50 fb for a mass of 1.5 TeV to about 1.0 fb for a mass of 5 TeV. Excited quarks are excluded below masses of 4.4 TeV, and non-thermal quantum black holes are excluded below masses of 3.8 (6.2) TeV for Randall–Sundrum (Arkani-Hamed–Dimopoulos–Dvali) models with one (six) extra dimensions.

© 2016 CERN for the benefit of the ATLAS Collaboration.

Reproduction of this article or parts of it is allowed as specified in the CC-BY-4.0 license.

Contents

1	Introduction	3
2	The ATLAS Detector	5
3	Data and simulation samples	6
4	Event selection	7
5	Signal and background models	9
	5.1 Signal model	10
	5.2 Background model	10
6	Systematic uncertainties	11
7	Statistical procedures of the excess search	12
8	Results	13
9	Conclusions	17

1 Introduction

Final states consisting of a photon and a jet (γ +jet) with large invariant mass could be produced in proton–proton (pp) collisions at the Large Hadron Collider (LHC) in many scenarios of physics beyond the Standard Model (SM), including decays of excited quarks (q^*) and non-thermal quantum black holes.

Excited-quark states with vector-like couplings to the SM particles [1, 2] may be produced in pp collisions via the fusion of a gluon with a quark and then decay promptly to a quark and a photon ($qg \rightarrow q^* \rightarrow q\gamma$). At a pp centre-of-mass energy of $\sqrt{s} = 13$ TeV, the expected leading-order (LO) q^* production cross sections ($pp \rightarrow q^* + X$) times the $q^* \rightarrow q\gamma$ decay branching ratios, combining all flavours of excited quarks and assuming a compositeness scale equal to the excited-quark mass m_{q^*} , are shown in figure 1 as a function of m_{q^*} . These cross sections were obtained with the PYTHIA 8.186 event generator [3]. Only gauge interactions like those in the SM are considered for the excited quarks, with the $SU(3)$, $SU(2)$, and $U(1)$ coupling multipliers fixed to $f_s = f = f' = 1$. The predicted production cross section times branching ratio is approximately 5 fb for $m_{q^*} = 4$ TeV.

Theories with n extra spatial dimensions, such as the Randall–Sundrum type-I (RS1) model [4] and the Arkani-Hamed–Dimopoulos–Dvali (ADD) model [5, 6], solve the mass hierarchy problem of the SM by lowering the fundamental scale M_* of quantum gravity (\tilde{M} in the RS1 model and M_D in the ADD model) to a few TeV. As a consequence, the LHC could produce quantum black holes (QBH) with masses near M_* [7, 8], which would then decay before thermalizing, producing low-multiplicity final states [9, 10]. The RS1 model studied in this article has $n = 1$ extra dimensions. For the ADD model, the same benchmark scenario ($n = 6$) is investigated as in the previous ATLAS publication [11]. In this article it is also assumed that the mass threshold for black hole production is equal to the Planck scale, $M_{\text{th}} = M_*$. The maximum mass for black hole production, which in any case cannot exceed the pp centre-of-mass energy, is set to $3M_*$ (when $M_* < \sqrt{s}/3$), to avoid the high-mass regime in which a classical description of the black hole should replace the quantum one. A continuum of black holes with invariant masses between the threshold mass and the maximum mass can therefore be produced, with a probability rapidly decreasing with the mass. The total expected production cross sections times decay branching ratios for $pp \rightarrow \text{QBH} + X \rightarrow \gamma + q/g + X$ as a function of the threshold mass, assuming that all QBHs decay to two-body final states and summing over all parton types in the initial and final state, are shown in figure 1. These cross sections were obtained with the QBH 2.02 event generator [12]. At $\sqrt{s} = 13$ TeV the predicted total production cross section times branching ratio is 1.4 fb (390 fb) for RS1 (ADD) black holes with $M_{\text{th}} = 4$ TeV.

Both the $q^* \rightarrow q\gamma$ and $\text{QBH} \rightarrow q\gamma, g\gamma$ decays (regardless of the number of extra dimensions) would yield final states with a photon and a jet having large transverse momenta and large invariant mass $m_{\gamma j}$. Such events would manifest themselves in the $m_{\gamma j}$ distribution as a broad peak above the steeply falling background from SM prompt γ + jet events [13, 14], typically produced by QCD Compton scattering ($qg \rightarrow q\gamma$).

In this article, a search for a localized, high-mass excess in the γ + jet invariant mass distribution is presented. The excess would arise from s -channel production of a resonant signal. The measurement uses 3.2 fb^{-1} of pp collisions collected at a centre-of-mass energy $\sqrt{s} = 13$ TeV by the ATLAS detector in 2015.

The results are interpreted in terms of the visible cross section (i.e. the product of the production cross section, the branching ratio, the detector acceptance and the selection efficiency) of a generic Gaussian-shaped signal with mass M_G and width σ_G . The results are also interpreted in terms of the cross section

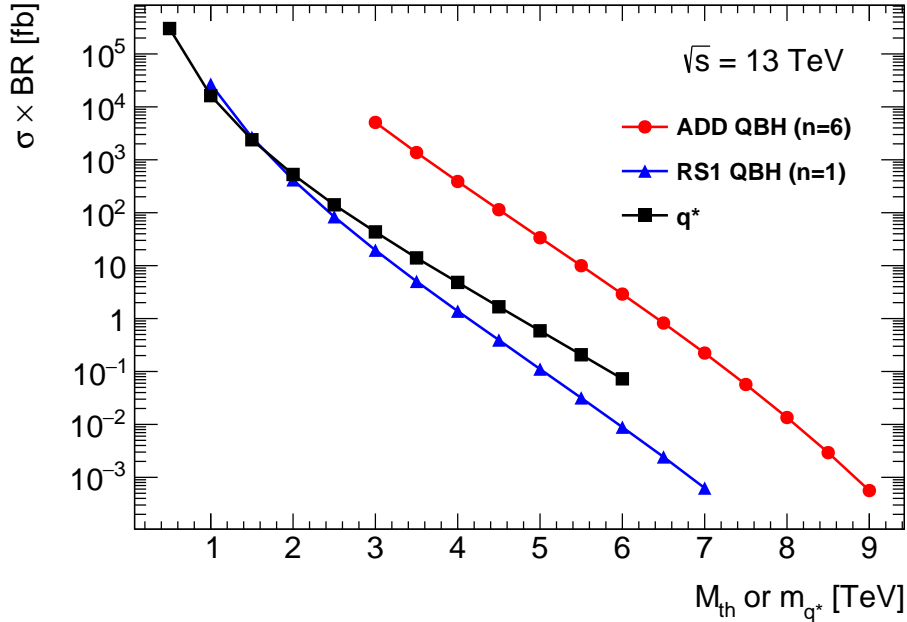


Figure 1: Production cross section times $\gamma + \text{jet}$ branching ratio for an excited quark q^* and two different non-thermal quantum black hole models (RS1, ADD) as a function of the q^* mass or the mass threshold for black hole production M_{th} , in pp collisions at $\sqrt{s} = 13$ TeV. The q^* cross section is computed at leading order in α_s with the PYTHIA 8.186 event generator [3]. The excited-quark model assumes that the compositeness scale is equal to the excited-quark mass m_{q^*} , and that gauge interactions of excited quarks are like those in the SM, with the $SU(3)$, $SU(2)$, and $U(1)$ coupling multipliers fixed to $f_s = f = f' = 1$. The quantum black hole cross sections are obtained with the QBH 2.02 event generator [12]. In the RS1 and ADD quantum black hole models the number of extra spatial dimensions is $n = 1$ and $n = 6$, respectively. The maximum mass for black hole production is set to the pp centre-of-mass energy or to $3M_{\text{th}}$ if $M_{\text{th}} < \sqrt{s}/3$. The cross sections are calculated in 0.5 GeV mass steps (dots) and interpolated with a continuous function (solid lines).

times branching ratio to a photon and a quark or a gluon in three benchmark models: a q^* state, a non-thermal RS1 QBH, and a non-thermal ADD QBH (for $n = 6$).

For the case of a Gaussian-shaped signal, the width σ_G is assumed to be proportional to M_G ; three possible values of σ_G/M_G are considered: 2%, 7% and 15%. The experimental photon+jet invariant mass resolution improves from 2.4% at 1 TeV to 1.5% at 6 TeV. The smallest value of σ_G/M_G (2%) thus corresponds to the typical photon+jet invariant mass resolution and hence represents the case of an intrinsically narrow resonance.

The RMS width of the q^* lineshape is expected to increase from about 250 GeV at $m_{q^*} = 1$ TeV to more than 1 TeV at $m_{q^*} = 6$ TeV and beyond. Quantum black holes are expected to produce even broader signals, due to the production of a continuum of QBHs with masses between the threshold mass M_{th} and the maximum mass.

Previous searches for generic Gaussian-shaped resonances, excited quarks, and ADD quantum black holes in the $\gamma + \text{jet}$ final state have been performed by the ATLAS and CMS collaborations using pp collisions at either $\sqrt{s} = 7$ TeV [15] or 8 TeV [11, 16]. No significant excess of events over the background was found, leading to lower limits on the mass of excited quarks at 3.5 TeV from both the ATLAS

and CMS experiments [11, 16] and on the ADD QBH mass at 4.6 TeV by ATLAS (for $n = 6$) [11]. No limits on RS1 quantum black holes with the photon+jet final state have been set so far. Using the dijet final state, ATLAS has set a lower limit on the q^* mass at 4.1 TeV and on the ADD QBH mass at 5.8 TeV for $n = 6$ [17], while CMS has excluded q^* masses below 3.3 TeV and ADD QBH masses below 4.0–5.3 TeV depending on n [18, 19]. ATLAS has also searched for quantum black hole production by looking for high-mass dilepton [20] and lepton+jet [21] resonances in $\sqrt{s} = 8$ TeV data.

Recently, using data collected at $\sqrt{s} = 13$ TeV, the ATLAS and CMS collaborations performed searches for excited quarks in dijet final states [22, 23], and ATLAS searched for quantum black holes in dijet final states [22] and for thermal black holes in multijet final states [24]. Excited quarks with masses below 5.2 TeV and RS1 or ADD ($n = 6$) quantum black holes with masses below 5.3 TeV and 8.3 TeV respectively, decaying to dijets, are excluded.

The searches presented in this article exploit analysis techniques and a selection strategy similar to those in a previous search using 20.3 fb^{-1} of pp collisions at $\sqrt{s} = 8$ TeV [11]. Despite the six times smaller integrated luminosity at $\sqrt{s} = 13$ TeV, the sensitivity of the present search to the q^* and QBH signals exceeds the exclusion limits obtained with 8 TeV data. This is due to the significant growth of the q^* and QBH production cross section with the increase of the pp centre-of-mass energy from 8 TeV to 13 TeV. For instance, for a mass of 5 TeV, the production cross sections rise by more than two orders of magnitude for both the q^* and QBHs, while the background cross section increases by less than an order of magnitude.

The article is organized as follows. In section 2 a brief description of the ATLAS detector is given. Section 3 summarizes the data and simulation samples used in this study. The event selection is discussed in section 4. The signal and background modelling are presented in section 5. The systematic uncertainties are described in section 6. In section 7, the signal search and limit-setting strategies are discussed, and finally the results are presented in section 8.

2 The ATLAS Detector

The ATLAS detector [25] is a multi-purpose particle detector with approximately forward-backward symmetric cylindrical geometry.¹ The inner tracking detector (ID) covers $|\eta| < 2.5$ and consists of a silicon pixel detector (including the newly installed innermost pixel layer [26]), a silicon microstrip detector, and a straw-tube transition radiation tracker. The ID is surrounded by a thin superconducting solenoid providing a 2 T axial magnetic field and by a high-granularity lead/liquid-argon (LAr) sampling electromagnetic (EM) calorimeter. The EM calorimeter measures the energy and the position of electromagnetic showers with $|\eta| < 3.2$. It includes a presampler (for $|\eta| < 1.8$) and three sampling layers, longitudinal in shower depth, up to $|\eta| = 2.5$. The hadronic calorimeter, surrounding the electromagnetic one and covering $|\eta| < 4.9$, is a sampling calorimeter which uses either scintillator tiles or LAr as the active medium, and steel, copper or tungsten as the absorber material. The muon spectrometer (MS) surrounds the calorimeters and consists of three large superconducting air-core toroid magnets, each with eight coils, a system of precision tracking chambers ($|\eta| < 2.7$), and fast tracking chambers ($|\eta| < 2.4$) for triggering.

¹ ATLAS uses a right-handed coordinate system with its origin at the nominal interaction point (IP) in the centre of the detector and the z -axis along the beam pipe. The x -axis points from the IP to the centre of the LHC ring, and the y -axis points upward. Cylindrical coordinates (r, ϕ) are used in the transverse plane, ϕ being the azimuthal angle around the z -axis. The pseudorapidity is defined in terms of the polar angle θ as $\eta = -\ln \tan(\theta/2)$.

Events containing photon candidates are selected by a two-level trigger system. The first-level trigger is hardware based; using a trigger cell granularity coarser than that of the EM calorimeter, it searches for electromagnetic clusters within a fixed window of size 0.2×0.2 in $\eta \times \phi$ and retains only those whose total transverse energy in two adjacent trigger cells is above a programmable threshold. The second, high-level trigger is implemented in software and employs algorithms similar to those used offline to identify jets and photon candidates. Such algorithms exploit the full granularity and precision of the calorimeter to refine the first-level trigger selection, based on the improved energy resolution and detailed information about energy deposition in the calorimeter cells.

3 Data and simulation samples

Data events were collected in pp collisions at $\sqrt{s} = 13$ TeV produced by the LHC in 2015. The average number of inelastic interactions per bunch crossing was 14. Only events taken in stable beam conditions and in which the trigger system, the tracking devices and the calorimeters were operational and with good data quality are considered. The integrated luminosity of the analysed data sample is $L_{\text{int}} = 3.2 \text{ fb}^{-1}$.

The events used for the analysis are recorded by a trigger requiring at least one photon candidate with transverse momentum above 140 GeV and passing loose identification requirements based on the shower shapes in the EM calorimeter and on the energy leaking into the hadronic calorimeter from the EM calorimeter [27].

Twelve samples of simulated $pp \rightarrow q^* + X \rightarrow \gamma + q + X$ events, with q^* masses in the range between 500 GeV and 6 TeV and separated by 500 GeV intervals, were generated at leading order in the strong coupling constant α_s with PYTHIA 8.186. The NNPDF 2.3 [28] parton distribution functions and the A14 set of tuned parameters [29] of the underlying event were used.

Simulated samples of QBHs decaying into a photon and a quark or a gluon were generated with QBH 2.02, interfaced to PYTHIA 8.186 for hadronization and simulation of the underlying event. The CTEQ6L1 [30] parton distribution functions and the A14 tune of the underlying event were used. Thirteen samples of $pp \rightarrow \text{QBH} + X \rightarrow \gamma + q/g + X$ events were produced for RS1 (ADD $n = 6$) quantum black holes with equally spaced M_{th} values between 1 (3) TeV and 7 (9) TeV, in 0.5 TeV steps.

To study the properties of the background, events from SM processes containing a photon with associated jets are simulated using the SHERPA 2.1.1 [31] generator, requiring a photon transverse momentum above 70 GeV. Matrix elements are calculated at LO with up to four partons and merged with the SHERPA parton shower [32] using the ME+PS@LO prescription [33]. The CT10 PDF set [34] is used in conjunction with a dedicated parton shower tuning developed by the SHERPA authors. The samples are binned in the photon transverse momentum, p_{T}^γ , to cover the full spectrum relevant to this analysis.

All the above Monte Carlo (MC) samples were passed through a detailed GEANT4 [35] simulation of the ATLAS detector response [36]. Moreover, additional inelastic pp interactions in the same and neighbouring bunch crossings, denoted as pile-up, are included in the event simulation by overlaying a number of minimum-bias events consistent with that observed in data. Multiple overlaid proton–proton collisions are simulated with the soft QCD processes of PYTHIA 8.186 using the A2 tune [37] and the MSTW2008LO PDF set [38].

Supplementary studies of the invariant mass shape of the $\gamma + \text{jet}$ background are also performed with the parton-level, next-to-leading-order (NLO) JETPHOX v1.3.1_2 generator [39] using the NNPDF 2.3 parton

distribution functions and the NLO photon fragmentation function [40]. The nominal renormalization, factorization and fragmentation scales are set to the photon transverse momentum. Jets of partons are reconstructed using the anti- k_t algorithm [41] with a radius parameter $R = 0.4$. The total transverse energy from partons produced inside a cone of size $\Delta R = \sqrt{(\Delta\eta)^2 + (\Delta\phi)^2} = 0.4$ around the photon is required to be lower than $2.45 \text{ GeV} + 0.022 \times p_T^\gamma$, to match the selection requirement described in the next section. Experimental effects (detector reconstruction efficiencies and resolution) as well as hadronization and pile-up are not taken into account in this sample.

4 Event selection

Each event is required to contain at least one primary vertex candidate with two or more tracks with $p_T > 400 \text{ MeV}$. The tracks must satisfy quality requirements based on the number of reconstructed intersections with the silicon pixel and strip detectors and the track impact parameters with respect to the centre of the luminous region. The primary vertex is defined as the candidate with the largest sum of the p_T^2 of the tracks that are considered to be associated to it, based on a requirement on a χ^2 variable calculated between the estimated vertex position and the point of closest approach of the track to the vertex.

Photons are reconstructed from energy deposits (clusters) found in the EM calorimeter by a sliding-window algorithm. The reconstruction algorithm looks for matches between energy clusters and tracks reconstructed in the inner detector and extrapolated to the calorimeter. Well-reconstructed clusters matched to tracks are classified as electron candidates while clusters without matching tracks are classified as unconverted photon candidates. Clusters matched to pairs of tracks that are consistent with the hypothesis of a $\gamma \rightarrow e^+e^-$ conversion process are classified as converted photon candidates. To maximize the reconstruction efficiency for electrons and photons, clusters matched to single tracks without hits in an active region of the innermost pixel layer are considered as electron candidates and as converted photon candidates. Both unconverted and converted photon candidate are used for the search presented in this paper.

The energies of the photon candidates are calibrated following the procedure described in ref. [42]. The calibration algorithm, tuned using 13 TeV event simulation, accounts for energy loss upstream of the EM calorimeter and for both lateral and longitudinal shower leakage. Correction factors are extracted from 8 TeV $Z \rightarrow ee$ data and simulated events reconstructed with the algorithms used in the 2015 data taking. Additional corrections and systematic uncertainties take into account the differences between the 2012 and 2015 configurations.

To reduce backgrounds from hadrons, photon candidates are required to fulfil η -dependent requirements consisting of nine independent selections, one on the hadronic leakage and eight on shower shape variables measured with the first two sampling layers of the electromagnetic calorimeter [27]. The requirements were optimized for the 2015 data-taking conditions using simulated samples of photons and hadronic jets produced in 13 TeV pp collisions. The simulation is corrected for the differences between $\sqrt{s} = 8 \text{ TeV}$ data and simulated events for each photon shower shape variable.

Groups of contiguous calorimeter cells (topological clusters) are formed based on the significance of the ratio of deposited energy to calorimeter noise. To further reduce background photons from hadronic jets, the transverse isolation energy $E_{T,\text{iso}}^\gamma$ of the photon candidates is required to be less than $2.45 \text{ GeV} + 0.022 \times p_T^\gamma$. This energy is computed from the sum of the energies of all cells belonging to topological

clusters and within a cone of $\Delta R = 0.4$ around the photon direction. The contributions from the underlying event and the pile-up [43, 44], as well as from the photon itself, are subtracted. The isolation requirement has a signal efficiency of about 98% over the whole photon transverse momentum range relevant to this analysis.

Jets are reconstructed from topological clusters of calorimeter cells using the anti- k_t algorithm with radius parameter $R = 0.4$. Jets affected by noise or hardware problems in the detector, or identified as arising from non-collision backgrounds, are discarded [45]. Jet four-momenta are computed by summing over the topological clusters that constitute each jet, treating each cluster as a four-vector with zero mass. To reduce the effects of pile-up on the jet momentum, an area-based subtraction method is employed [43, 44]. Jet energies are then calibrated by using corrections from the simulation and scale factors determined in various control samples ($\gamma + \text{jet}$, $Z + \text{jet}$ and multijet events) in 8 TeV data [46] and validated with early 2015 data [47]. These corrections are applied to 2015 data, after taking into account in the simulation the changes in the detector and in the data-taking conditions between 8 TeV and 13 TeV data, and propagating as systematic uncertainties those related to this extrapolation procedure. Jets with $p_T < 20$ GeV or within $\Delta R = 0.2$ (0.4) of a well-identified and isolated electron (photon) with transverse momentum above 25 GeV are not considered.

Events are selected if they contain at least one photon candidate and at least one jet candidate satisfying all the previous criteria and each having $p_T > 150$ GeV. The photon trigger has an efficiency of $(99.9^{+0.1}_{-1.3})\%$ for these events. The trigger efficiency is measured in data as the product of the efficiency of the high-level trigger computed from events selected by the first-level trigger and the efficiency of the first-level trigger with respect to offline identification [48].

Since t -channel $\gamma + \text{jet}$ and dijet production rates increase while the rate of the s -channel signal production decreases with the photon and jet absolute pseudorapidity, photons are required to be in the barrel calorimeter, $|\eta^\gamma| < 1.37$. Moreover, as a consequence of the different production mechanisms for the signal and background, the pseudorapidity separation $\Delta\eta$ between the photon and the jet candidates tend to be smaller for the signal than for the background, particularly for large values of the photon–jet invariant mass. For this reason, events with $|\Delta\eta| > 1.6$ are discarded.

In events in which more than one good photon or jet candidate is found, the highest- p_T candidate of each type is selected to form the resonant $\gamma + \text{jet}$ candidate. Events in which the angular separation between the photon and any jet with $p_T > 30$ GeV (after the jet–photon overlap removal) is $\Delta R < 0.8$ are discarded. This requirement suppresses background events from SM photon+jet production in which the photon is emitted at large angles in the fragmentation of a quark or a gluon.

The total signal efficiency (including detector acceptance) depends on the resonant mass of the hypothetical signal, and is described in the next section. The product of acceptance times efficiency for the QBH and q^* signals and a resonance mass of 3 TeV is close to 50%.

There are 2603 candidates in the data sample passing the full event selection and having invariant mass above 1 TeV. The $\gamma + \text{jet}$ candidate with the highest $m_{\gamma j}$ value has an invariant mass of 2.87 TeV. A small contamination from dijet events is expected, due to jets misidentified as photons in the calorimeter. Such fake candidates typically arise from jets containing a neutral meson (most likely a π^0) carrying a large fraction of the jet energy and decaying into two collimated photons. These candidates are on average less isolated from activity in the neighbouring cells of the calorimeters and have on average wider shower shapes in the electromagnetic calorimeter. The purity of true photon+jet events in the selected sample is estimated to be around 93% by means of a two-dimensional sideband method based on the numbers of photon+jet candidates in which the photon either passes anti-isolation requirements, anti-identification

requirements, or both [27], thus indicating that the dijet contamination is rather small. For the purity measurement a photon candidate is considered non-isolated if its isolation transverse energy is at least 3 GeV larger than the maximum allowed $E_{T,iso}^\gamma$ for a photon to be regarded as isolated. A photon candidate is non-identified if it fails at least one of the requirements on four shower shape variables computed from the energy deposited in the finely segmented cells of the first layer of the electromagnetic calorimeter. No evidence of a dependence of the photon purity on the γ + jet invariant mass is observed.

Figure 2 shows the comparison between the $m_{\gamma j}$ distribution of events selected in data and the shapes predicted by SHERPA and JETPHOX for SM γ + jet production, neglecting the dijet contribution. The bin width rises from 100 GeV to 300 GeV with increasing $m_{\gamma j}$, to account for the corresponding decrease in the number of data events and increase in the intrinsic width of most of the signals considered in this study. The simulated spectra from SHERPA and JETPHOX are normalized to the data in the range $0.5 \text{ TeV} < m_{\gamma j} < 2.5 \text{ TeV}$. The shapes of the $m_{\gamma j}$ distributions in data and simulation agree in the range studied. The agreement is better for SHERPA, due to the inclusion of hadronization and underlying-event effects and of the detector response.

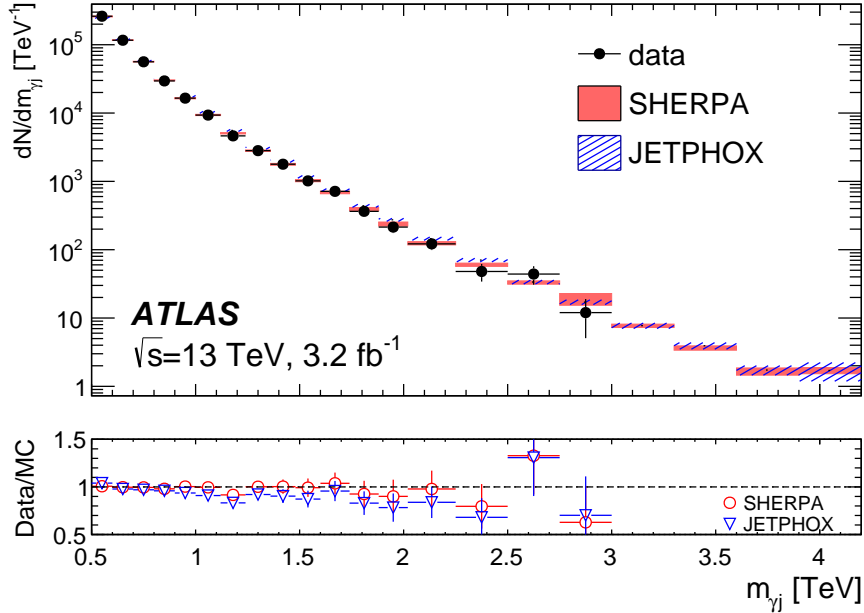


Figure 2: Photon–jet invariant mass spectrum in data (black dots) compared to the shape predicted by a γ +jet parton-level calculation (JETPHOX, hatched blue bands) and a parton-shower simulation (SHERPA, solid red bands). Both predictions are normalized to data in the range $0.5 \text{ TeV} < m_{\gamma j} < 2.5 \text{ TeV}$. The number of events in each bin is normalised by the bin width. In the bottom panel the ratios of the data to the two predictions are shown. Statistical uncertainties due to the size of the data and simulated samples and systematic uncertainties for simulations are shown.

5 Signal and background models

In order to evaluate the strength of a possible contribution of a signal originating from physics beyond the SM, an unbinned maximum-likelihood fit of the signal+background model to the $m_{\gamma j}$ distribution of the

selected data events is performed.

5.1 Signal model

The signal model consists of the expected $m_{\gamma j}$ distribution after reconstruction and selection (called *template* in the following) for each type of signal under study and as a function of its hypothetical mass M (M_G , m_{q^*} or M_{th} depending on the signal type).

The model is the product $f_{\text{sig}}(m_{\gamma j}) \times (\sigma \times BR) \times (A \times \varepsilon) \times L_{\text{int}}$ of a template $f_{\text{sig}}(m_{\gamma j})$ with the production cross section times the branching ratio to a photon and a quark or a gluon, $\sigma \times BR$, the expected acceptance times efficiency, $A \times \varepsilon$, and the integrated luminosity of the sample, L_{int} .

In the case of a generic Gaussian-shaped signal with mass M_G and an arbitrary production cross section, the template is a simple Gaussian distribution centred at M_G with a width σ_G proportional to the mass; three possible values of σ_G/M_G are considered (2%, 7%, 15%). The results are directly interpreted in terms of the visible cross section $\sigma \times BR \times A \times \varepsilon$, which is the parameter of interest in the maximum-likelihood fit described in section 7.

For the other three types of signal (q^* , RS1 QBH, ADD QBH), the parameter of interest in the fit is the product $\sigma \times BR$. The normalized $m_{\gamma j}$ template for the generated signals (section 3) is obtained via smoothing with a kernel density estimation technique [49, 50]. The normalized distributions of the invariant masses of the candidates passing the full selection in the simulated signal samples are used. For intermediate masses where generated samples are not available, the $m_{\gamma j}$ distribution is obtained by a moment-morphing method [51]. The product of acceptance times efficiency $A \times \varepsilon$ for q^* and QBH signals for each mass M is obtained through a continuous interpolation of the values obtained from the simulation of the signal samples generated at discrete mass points (section 3). The interpolating function is a third-order spline. The acceptance times efficiency curves as a function of M are rather similar for the three models, increasing between $M = 1$ TeV ($A \times \varepsilon \approx 46\%$) and $M = 4$ TeV ($A \times \varepsilon \approx 51\%$), beyond which it slowly decreases ($A \times \varepsilon \approx 47\%$ at 9 TeV).

5.2 Background model

The background $m_{\gamma j}$ template is the same four-parameter ansatz function [52] as used in previous searches for high-mass resonances in the $\gamma + \text{jet}$ final state [11, 15]:

$$f_{\text{bkg}}(x \equiv m_{\gamma j} / \sqrt{s}) = p_0(1-x)^{p_1} x^{-p_2-p_3 \log x}. \quad (1)$$

The parameters of this empirical function, as well as the total background yield, are directly extracted from the final fit to the data with the signal+background model.

The possible bias in the fitted signal due to choosing this functional form is estimated through signal+background fits to large $\gamma + \text{jet}$ background samples generated with JETPHOX, and included in the systematic uncertainties, as described in section 6. The small contamination from dijet events is neglected, since the photon–jet purity of the sample is high (around 93%) and does not depend significantly on $m_{\gamma j}$. Detector effects are considered by reweighting the JETPHOX sample with corrections obtained from the SHERPA photon–jet simulation, as explained in the next section.

The range for the fit is chosen in order to have a large efficiency for the signal and to provide a sufficiently wide mass sideband. The mass sideband should be wide enough to determine from the data the parameters of the background model with good precision, but not too wide in order to suppress as much as possible any bias in the signal. The bias is considered acceptable if it is less than 10% of the expected signal yield or less than 20% of the expected statistical uncertainty of the background. The chosen ranges are $1 \text{ TeV} < m_{\gamma j} < 5.5 \text{ TeV}$ in the searches for generic Gaussian-shaped resonances, q^* , or RS1 QBH, and $2 \text{ TeV} < m_{\gamma j} < 8 \text{ TeV}$ in the ADD QBH search. These ranges probe signals with masses between 1.5 and 5 TeV (Gaussian-shaped resonances, q^* , RS1 QBH), or between 3 and 7 TeV (ADD QBH).

A further test to check whether the chosen ansatz function accurately describes the expected background distribution is performed by fitting pseudo-data generated from the simulated SHERPA photon+jet events with alternative functions with more degrees of freedom. An F -test is then performed to compare the χ^2 used to estimate the goodness of the nominal fit to the χ^2 of the alternative fit. No significant decrease of the χ^2 was observed when adding more degrees of freedom to the ansatz function used as the nominal background model.

6 Systematic uncertainties

The systematic uncertainty of the integrated luminosity is $\pm 5\%$. It is derived, following a methodology similar to that detailed in ref. [53], from a preliminary calibration of the luminosity scale using x - y beam-separation scans performed in August 2015.

For the q^* and QBH signals, the acceptance times efficiency is subject to systematic uncertainties in the trigger efficiency ($^{+0.1}_{-1.3}\%$), photon identification efficiency ($\pm 2\%$ to $\pm 4\%$) and photon isolation efficiency ($\pm 1\%$). The systematic uncertainty on the trigger efficiency is estimated as the difference between the efficiency measured in data and the efficiency obtained in MC simulations. It is dominated by the statistical uncertainty of the measurement in data. The photon identification and isolation efficiency uncertainties are estimated conservatively by recomputing the signal efficiency after removing the MC-to-data corrections from the shower shape variables and the transverse isolation energy.

Additional uncertainties in the signal arise from the uncertainties in the photon and jet energy scales and resolutions as a consequence of the requirements placed on the photon and jet transverse momenta and invariant mass. The energy scale and resolution uncertainties have effects on $A \times \epsilon$ that are smaller than $\pm 0.5\%$ for photons (and are thus neglected) and are about $\pm 1\%$ to $\pm 2\%$ (energy scale) and $\pm 1\%$ (energy resolution) for jets. These uncertainties have a negligible impact on the signal $m_{\gamma j}$ distribution since the intrinsic width dominates over the experimental resolution and is much larger than the possible bias arising from the photon and jet energy scale uncertainties. The limited size of the simulated signal samples yields an uncertainty in the signal efficiency of $\pm 1\%$. Systematic uncertainties in the signal acceptance and shape due to the PDF uncertainties were examined and found to be negligible compared to the other uncertainties.

The background yield and values for the parameters of its invariant mass distribution are directly extracted from a fit to the data. A possible systematic uncertainty in the signal yield arises from the choice of functional form used to model the background distribution. In order to estimate this uncertainty, a large γ + jet background sample (about seven billion events) is generated using JETPHOX and fit with the full signal+background model. This is done for each tested signal model and mass M . The photon and jet

kinematic requirements described in section 4 are applied. Since no signal is present in these background-only samples, the resulting number of spurious signal events from the fit, $N_{\text{spur}}(M) = \sigma_{\text{spur}}^{\text{eff}}(M) \times L_{\text{int}}$ for the Gaussian-shaped signal and $N_{\text{spur}}(M) = \sigma_{\text{spur}}^{\text{eff}}(M) \times (A \times \varepsilon)(M) \times L_{\text{int}}$ for the other signal models, is taken as an estimate of the bias for the model under test. In order to cover possible uncertainties in the JETPHOX prediction itself, the fit is repeated after varying each of several model parameters and estimating reconstruction effects. The final uncertainty is thus the largest spurious signal cross section obtained when doing the signal+background fits to the following background-only samples:

- the nominal sample generated with JETPHOX;
- the samples generated with JETPHOX after varying the eigenvalues of the NNPDF 2.3 set by $\pm 1\sigma$;
- the samples generated with JETPHOX after varying the value of the strong coupling constant by ± 0.002 around the nominal value of 0.018;
- the samples generated with JETPHOX after varying the renormalization, factorization and fragmentation scales between half and twice the photon transverse momentum;
- the sample obtained after reweighting the JETPHOX $m_{\gamma j}$ distribution by the ratio of the reconstructed and particle-level $m_{\gamma j}$ spectra predicted by SHERPA.

All samples are rescaled so that the total number of events is equal to the number observed in the data. For the Gaussian signal search, the spurious cross section $\sigma_{\text{spur}}^{\text{eff}}(M)$ varies between 10 fb at 1 TeV and less than 0.1 fb at 5.5 TeV. The estimated spurious signal yield $N_{\text{spur}}(M)$ varies between 3×10^{-3} and 10% of the expected q^* yield for masses between 1.5 TeV and 5 TeV, between 5×10^{-4} and 10% of the expected RS1 QBH yield for masses between 1.5 TeV and 5 TeV, and between 5×10^{-5} and 3×10^{-3} of the expected ADD QBH yield for masses between 3 TeV and 7 TeV.

7 Statistical procedures of the excess search

To search for an excess over the SM background in the $m_{\gamma j}$ distribution in the data, quantify its significance and set limits, the profile-likelihood-ratio method described in ref. [54] is used. The extended likelihood function \mathcal{L} is built from the number n of observed events, the expected event yield N , and the functions f_{sig} and f_{bkg} describing the signal and background $m_{\gamma j}$ distributions:

$$\mathcal{L} = \text{Pois}(n|N(\theta)) \prod_{i=1}^n f(m_{\gamma j}^i, \theta) \times G(\theta). \quad (2)$$

In this expression $f(m_{\gamma j}^i, \theta)$ is the value of the probability density function (pdf) of the invariant mass distribution for each candidate event i , θ represents the nuisance parameters and $G(\theta)$ is a set of constraints on some of the nuisance parameters, as described in the following.

The number of expected candidates N is the sum of the number of signal events, the number of background candidates N_{bkg} , and the spurious signal yield $N_{\text{spur}}(M)$ fitted on background-only samples as described in the previous section. For the Gaussian-shaped signal, N is thus:

$$N = (\sigma \times BR \times A \times \varepsilon)(M) \times L_{\text{int}} + N_{\text{bkg}} + N_{\text{spur}}(M) \times \theta_{\text{spur}}, \quad (3)$$

while for the QBH and q^* signals it is:

$$N = (\sigma \times BR)(M) \times (A \times \varepsilon)(\theta^{\text{yield}}, M) \times L_{\text{int}} + N_{\text{bkg}} + N_{\text{spur}}(M) \times \theta_{\text{spur}}. \quad (4)$$

Here θ^{yield} are the nuisance parameters that implement the systematic uncertainties affecting the signal yields and θ_{spur} is the nuisance parameter corresponding to the systematic uncertainty from the choice of background model.

The total pdf $f(m_{\gamma j})$ is then:

$$f(m_{\gamma j}^i) = \frac{1}{N} \left[\left((\sigma \times BR \times A \times \varepsilon)(M) + \sigma_{\text{spur}}^{\text{eff}}(M) \times \theta_{\text{spur}} \right) \times L_{\text{int}} \times f_{\text{sig}}(m_{\gamma j}^i) + N_{\text{bkg}} \times f_{\text{bkg}}(m_{\gamma j}^i) \right] \quad (5)$$

for the Gaussian-shaped signal search and:

$$f(m_{\gamma j}^i) = \frac{1}{N} \left[\left((\sigma \times BR)(M) + \sigma_{\text{spur}}^{\text{eff}}(M) \times \theta_{\text{spur}} \right) \times (A \times \varepsilon)(\theta^{\text{yield}}, M) \times L_{\text{int}} \times f_{\text{sig}}(m_{\gamma j}^i) + N_{\text{bkg}} \times f_{\text{bkg}}(m_{\gamma j}^i) \right] \quad (6)$$

for the QBH and q^* searches, where f_{sig} and f_{bkg} are the signal and background templates, respectively.

Apart from the spurious signal, systematic uncertainties with an estimated size δ are incorporated into the likelihood by multiplying the relevant parameter of the statistical model by a factor $F_G(\delta, \theta) = (1 + \delta \cdot \theta)$ in the case of a Gaussian or, for cases where a negative model parameter does not make physical sense, by $F_{\text{LN}}(\delta, \theta) = e^{\delta \theta}$ for a log-normal pdf. In both cases the likelihood is multiplied by a constraint term $G(\theta)$ which is a standard normal distribution for θ , centred at zero.

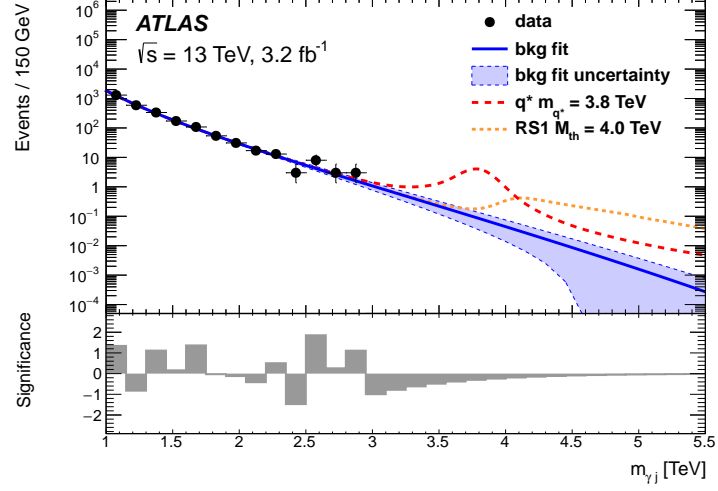
The significance of the signal is estimated by computing p_0 , which is defined as the p -value that quantifies the compatibility of the data with the background-only hypothesis. Upper limits on the signal cross section times branching ratio at 95% confidence level (CL) are set using a modified frequentist (CL_s) method [55], by identifying the value of $\sigma \times BR$ (or $\sigma \times BR \times A \times \varepsilon$ for the Gaussian-shaped resonance) for which CL_s is equal to 0.05. Due to the vanishingly small size of the selected dataset and of the expected background at masses beyond 2.8 TeV, the results are computed using ensemble tests.

8 Results

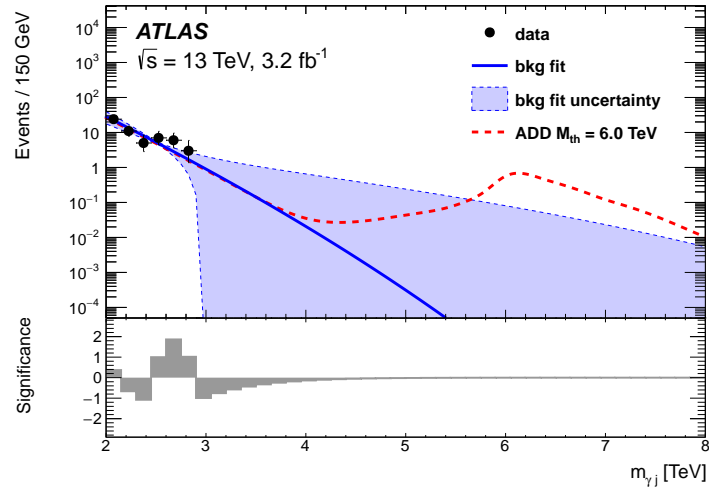
The data distributions in the $m_{\gamma j}$ regions used for the final fits are shown in figure 3. The background-only fit is overlaid, together with the expected distribution for a few signal models. The signal+background fits performed on the data show no significant excess of events. The smallest p_0 is obtained for a mass M equal to 2.6 TeV and corresponds to a significance of about 1.7σ .

Since no significant deviation from the background-only hypothesis is observed, upper limits are set on the visible cross section of a generic Gaussian-shaped signal and on the production cross section times branching ratio of excited quarks and quantum black holes.

The observed and expected upper limits on the visible cross sections for a generic Gaussian-shaped signal are shown in figure 4. The data exclude resonances with a mass of 1.5 TeV and visible cross sections above about 6 (50) fb, and resonances with a mass of 5 TeV and cross sections above about 0.8 (1.0) fb, for $\sigma_G/M_G = 2\%$ (15%).



(a)



(b)

Figure 3: Photon-jet invariant mass distributions of events selected in data and results of a background-only fit, for (a) the q^* and RS1 ($n = 1$) QBH searches and (b) the ADD ($n = 6$) QBH search. The top panels show the data (dots), the nominal fit results (blue lines), and the uncertainty on the background models (light blue bands) due to the uncertainty in the fit parameter values. Some examples of expected signals overlaid on the fitted background are also shown, for (a) a q^* with a mass of 3.8 TeV (red dashed line) and an RS1 ($n = 1$) QBH with a threshold mass of 4 TeV (orange dotted line) and (b) an ADD ($n = 6$) QBH with a threshold mass of 6 TeV (red dashed line). The bottom panels show the difference between the data and the prediction of the background-only fit, divided by the square root of the predicted background.

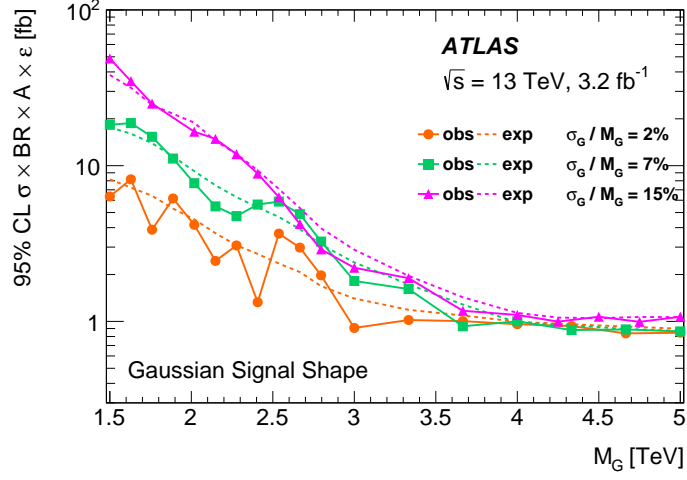
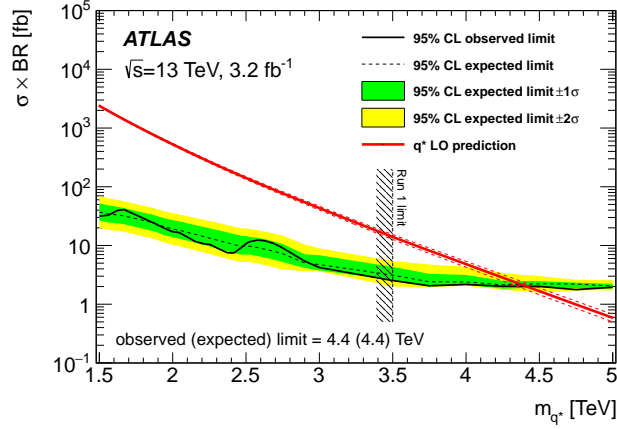


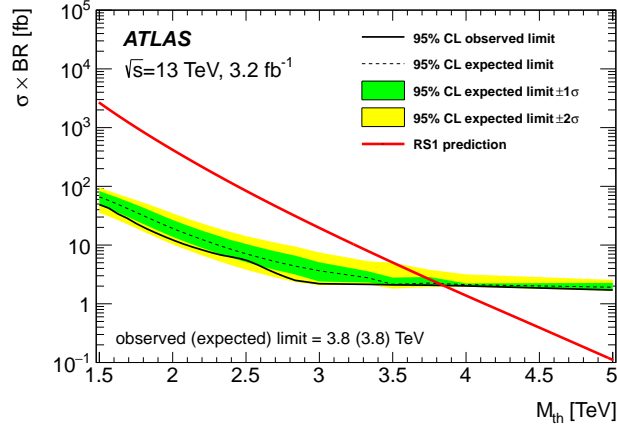
Figure 4: Observed (solid lines) and expected (dashed lines) 95% CL limits on the visible cross section ($\sigma \times BR \times A \times \epsilon$) for a hypothetical signal with a Gaussian-shaped $m_{\gamma j}$ distribution as a function of the signal mass M_G for three values of the width-to-mass ratio σ_G/M_G .

The observed and expected upper limits on the production cross sections times branching ratio to a photon and a quark or a gluon for benchmark models of excited quarks, RS1 QBHs and ADD QBHs are shown in figure 5.

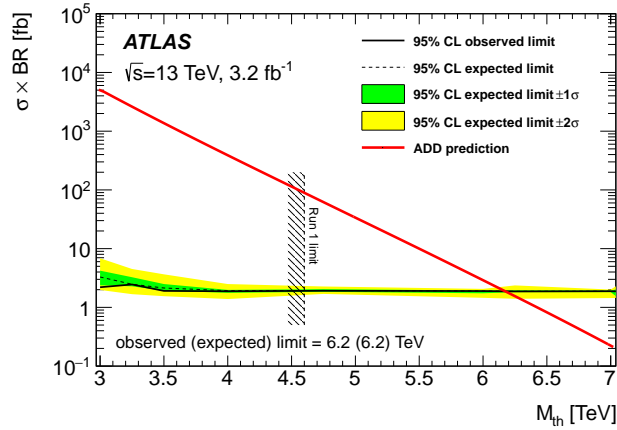
Comparing the measured upper limits to the theoretical predictions as a function of the mass of the resonance, lower limits are set for the excited-quark mass at 4.4 TeV and for the RS1 (ADD) quantum black hole mass at 3.8 (6.2) TeV. The uncertainty in the q^* theoretical cross section arising from PDF uncertainties reduces the maximum excluded mass by 1.5%. The limits on the q^* and ADD QBH mass improve on the ATLAS results at $\sqrt{s} = 8$ TeV in this channel by 0.9 TeV and 1.7 TeV, respectively.



(a)



(b)



(c)

Figure 5: Observed 95% CL limits (dots and solid black line) on the production cross section times branching ratio to a photon and a quark or a gluon for (a) an excited quark q^* , (b) an RS1 ($n = 1$) QBH, and (c) an ADD ($n = 6$) QBH. The limits are shown as a function of the q^* mass or the QBH production threshold mass. The median expected 95% CL exclusion limits (dashed line), in the case of no expected signal, are also shown. The green and yellow bands correspond to the $\pm 1\sigma$ and $\pm 2\sigma$ intervals. The red solid lines show the predicted $\sigma \times BR$ (at leading order in α_s in the case of the q^* model). The dashed red lines in (a) show how the PDF uncertainties affect the prediction. In the case of the q^* and ADD QBH searches, the corresponding limits from the ATLAS Run 1 pp data are indicated (vertical line).

9 Conclusions

A search for phenomena beyond the Standard Model has been performed using photon+jet events in 3.2 fb^{-1} of proton–proton collisions with a centre-of-mass energy of $\sqrt{s} = 13 \text{ TeV}$ collected by the ATLAS detector at the Large Hadron Collider. No significant excess in the $\gamma + \text{jet}$ invariant mass distribution was found with respect to a data-driven estimate of the smoothly falling distribution predicted by the Standard Model.

Limits at 95% CL using a profile likelihood method are obtained for three signal processes. They include (i) generic signals yielding a Gaussian lineshape, with intrinsic width between 2% and 15% of the resonance mass; (ii) excited quarks with vector-like couplings to Standard Model particles and a compositeness scale equal to their mass, and (iii) non-thermal quantum black holes in a type-1 Randall–Sundrum model with one extra spatial dimension, and in a Arkani-Hamed–Dimopoulos–Dvali model with six extra spatial dimensions. The limits on Gaussian-shaped resonances exclude 1.5 TeV resonances with visible cross sections above about 6 (50) fb and 5 TeV resonances with visible cross sections above about 0.8 (1.0) fb at $\sqrt{s} = 13 \text{ TeV}$ for $\sigma_G/M_G = 2\%$ (15%). Excited quarks are excluded for masses up to 4.4 TeV. Non-thermal RS1 and ADD quantum black hole models are excluded for masses up to 3.8 TeV and 6.2 TeV, respectively.

The limits on the excited quarks and the non-thermal quantum black holes are the most stringent limits set to date in the $\gamma + \text{jet}$ final state and supersede the previous ATLAS results at $\sqrt{s} = 8 \text{ TeV}$.

Acknowledgements

We thank CERN for the very successful operation of the LHC, as well as the support staff from our institutions without whom ATLAS could not be operated efficiently.

We acknowledge the support of ANPCyT, Argentina; YerPhI, Armenia; ARC, Australia; BMWFW and FWF, Austria; ANAS, Azerbaijan; SSTC, Belarus; CNPq and FAPESP, Brazil; NSERC, NRC and CFI, Canada; CERN; CONICYT, Chile; CAS, MOST and NSFC, China; COLCIENCIAS, Colombia; MSMT CR, MPO CR and VSC CR, Czech Republic; DNRF, DNSRC and Lundbeck Foundation, Denmark; IN2P3-CNRS, CEA-DSM/IRFU, France; GNSF, Georgia; BMBF, HGF, and MPG, Germany; GSRT, Greece; RGC, Hong Kong SAR, China; ISF, I-CORE and Benoziyo Center, Israel; INFN, Italy; MEXT and JSPS, Japan; CNRST, Morocco; FOM and NWO, Netherlands; RCN, Norway; MNiSW and NCN, Poland; FCT, Portugal; MNE/IFA, Romania; MES of Russia and NRC KI, Russian Federation; JINR; MESTD, Serbia; MSSR, Slovakia; ARRS and MIZŠ, Slovenia; DST/NRF, South Africa; MINECO, Spain; SRC and Wallenberg Foundation, Sweden; SERI, SNSF and Cantons of Bern and Geneva, Switzerland; MOST, Taiwan; TAEK, Turkey; STFC, United Kingdom; DOE and NSF, United States of America. In addition, individual groups and members have received support from BCKDF, the Canada Council, CANARIE, CRC, Compute Canada, FQRNT, and the Ontario Innovation Trust, Canada; EPLANET, ERC, FP7, Horizon 2020 and Marie Skłodowska-Curie Actions, European Union; Investissements d’Avenir Labex and Idex, ANR, Region Auvergne and Fondation Partager le Savoir, France; DFG and AvH Foundation, Germany; Herakleitos, Thales and Aristeia programmes co-financed by EU-ESF and the Greek NSRF; BSF, GIF and Minerva, Israel; BRF, Norway; the Royal Society and Leverhulme Trust, United Kingdom.

The crucial computing support from all WLCG partners is acknowledged gratefully, in particular from CERN and the ATLAS Tier-1 facilities at TRIUMF (Canada), NDGF (Denmark, Norway, Sweden), CC-IN2P3 (France), KIT/GridKA (Germany), INFN-CNAF (Italy), NL-T1 (Netherlands), PIC (Spain), ASGC (Taiwan), RAL (UK) and BNL (USA) and in the Tier-2 facilities worldwide.

References

- [1] S. Bhattacharya et al.,
Quark Excitations Through the Prism of Direct Photon Plus Jet at the LHC,
Phys. Rev. **D80** (2009) 015014, arXiv:0901.3927 [hep-ph].
- [2] U. Baur, M. Spira and P. M. Zerwas, *Excited-quark and -lepton production at hadron colliders*,
Phys. Rev. **D42** (1990) 815.
- [3] T. Sjöstrand, S. Mrenna, P. Skands, *A brief introduction to PYTHIA 8.1*,
Comput. Phys. Commun. **178** (2008) 852, arXiv:0710.3820 [hep-ph].
- [4] L. Randall and R. Sundrum, *A Large mass hierarchy from a small extra dimension*,
Phys. Rev. Lett. **83** (1999) 3370, arXiv:hep-ph/9905221.
- [5] N. Arkani-Hamed, S. Dimopoulos and G. Dvali,
The Hierarchy problem and new dimensions at a millimeter, *Phys. Lett.* **B429** (1998) 263,
arXiv:hep-ph/9803315.
- [6] I. Antoniadis et al., *New dimensions at a millimeter to a Fermi and superstrings at a TeV*,
Phys. Lett. **B436** (1998) 257, arXiv:hep-ph/9804398.
- [7] S. Dimopoulos and G. L. Landsberg, *Black holes at the LHC*, *Phys. Rev. Lett.* **87** (2001) 161602,
arXiv:hep-ph/0106295.
- [8] S. B. Giddings and S. D. Thomas,
High-energy colliders as black hole factories: The End of short distance physics,
Phys. Rev. **D65** (2002) 056010, arXiv:hep-ph/0106219.
- [9] X. Calmet, W. Gong and S. D. Hsu, *Colorful quantum black holes at the LHC*,
Phys. Lett. **B668** (2008) 20, arXiv:0806.4605 [hep-ph].
- [10] D. M. Gingrich, *Quantum black holes with charge, colour, and spin at the LHC*,
J. Phys. **G37** (2010) 105008, arXiv:0912.0826 [hep-ph].
- [11] ATLAS Collaboration, *Search for new phenomena in photon+jet events collected in
proton-proton collisions at $\sqrt{s} = 8$ TeV with the ATLAS detector*, *Phys. Lett. B* **728** (2014) 562,
arXiv:1309.3230 [hep-ex].
- [12] D. M. Gingrich,
Monte Carlo event generator for black hole production and decay in proton-proton collisions,
Comput. Phys. Commun. **181** (2010) 1917, arXiv:0911.5370 [hep-ph].
- [13] ATLAS Collaboration, *Measurement of the production cross section of an isolated photon
associated with jets in proton-proton collisions at $\sqrt{s} = 7$ TeV with the ATLAS detector*,
Phys. Rev. **D85** (2012) 092014, arXiv:1203.3161 [hep-ex].
- [14] ATLAS Collaboration, *Dynamics of isolated-photon plus jet production in pp collisions at
 $\sqrt{s} = 7$ TeV with the ATLAS detector*, *Nucl. Phys.* **B875** (2013) 483, arXiv:1307.6795 [hep-ex].

- [15] ATLAS Collaboration, *Search for production of resonant states in the photon-jet mass distribution using pp collisions at $\sqrt{s} = 7$ TeV collected by the ATLAS detector*, *Phys. Rev. Lett.* **108** (2012) 211802, arXiv:1112.3580 [hep-ex].
- [16] CMS Collaboration, *Search for excited quarks in the γ +jet final state in proton-proton collisions at $\sqrt{s} = 8$ TeV*, *Phys. Lett.* **B738** (2014) 274, arXiv:1406.5171 [hep-ex].
- [17] ATLAS Collaboration, *Search for new phenomena in the dijet mass distribution using pp collision data at $\sqrt{s} = 8$ TeV with the ATLAS detector*, *Phys. Rev.* **D91** (2015) 052007, arXiv:1407.1376 [hep-ex].
- [18] CMS Collaboration, *Search for narrow resonances and quantum black holes in inclusive and b-tagged dijet mass spectra from pp collisions at $\sqrt{s} = 7$ TeV*, *JHEP* **01** (2013) 013, arXiv:1210.2387 [hep-ex].
- [19] CMS Collaboration, *Search for narrow resonances using the dijet mass spectrum in pp collisions at $\sqrt{s} = 8$ TeV*, *Phys. Rev.* **D87** (2013) 114015, arXiv:1302.4794 [hep-ex].
- [20] ATLAS Collaboration, *Search for high-mass dilepton resonances in pp collisions at collisions at $\sqrt{s} = 8$ TeV with the ATLAS detector*, *Phys. Rev.* **D90** (2014) 052005, arXiv:1405.4123 [hep-ex].
- [21] ATLAS Collaboration, *Search for Quantum Black Hole Production in High-Invariant-Mass Lepton+Jet Final States Using pp Collisions at $\sqrt{s} = 8$ TeV and the ATLAS Detector*, *Phys. Rev. Lett.* **112** (2014) 091804, arXiv:1311.2006 [hep-ex].
- [22] ATLAS Collaboration, *Search for New Phenomena in Dijet Mass and Angular Distributions with the ATLAS Detector at $\sqrt{s} = 13$ TeV*, submitted to *Phys. Lett. B* (2015), arXiv:1512.01530 [hep-ex].
- [23] CMS Collaboration, *Search for narrow resonances decaying to dijets in proton-proton collisions at $\sqrt{s} = 13$ TeV* (2015), arXiv:1512.01224 [hep-ex].
- [24] ATLAS Collaboration, *Search for strong gravity in multijet final states produced in pp collisions at $\sqrt{s} = 13$ TeV using the ATLAS detector at the LHC*, submitted to *JHEP* (2015), arXiv:1512.02586 [hep-ex].
- [25] ATLAS Collaboration, *The ATLAS Experiment at the CERN Large Hadron Collider*, *JINST* **3** (2008) S08003.
- [26] ATLAS Collaboration, *ATLAS Insertable B-Layer Technical Design Report*, ATLAS-TDR-19, CERN-LHCC-2010-013 (2010), URL: <https://cds.cern.ch/record/1291633>.
- [27] ATLAS Collaboration, *Measurement of the inclusive isolated prompt photon cross section in pp collisions at $\sqrt{s} = 7$ TeV with the ATLAS detector*, *Phys. Rev.* **D83** (2011) 052005, arXiv:1012.4389 [hep-ex].
- [28] R. D. Ball et al., *Parton distributions with LHC data*, *Nucl. Phys.* **B867** (2013) 244, arXiv:1207.1303 [hep-ph].
- [29] ATLAS Collaboration, *ATLAS Run 1 Pythia8 tunes*, ATL-PHYS-PUB-2014-021 (2014), URL: <https://cds.cern.ch/record/1966419>.

- [30] J. Pumplin et al., *New generation of parton distributions with uncertainties from global QCD analysis*, **JHEP** **07** (2002) 012.
- [31] T. Gleisberg et al., *Event generation with SHERPA 1.1*, **JHEP** **02** (2009) 007, arXiv:0811.4622 [hep-ph].
- [32] S. Schumann and F. Krauss, *A Parton shower algorithm based on Catani-Seymour dipole factorisation*, **JHEP** **03** (2008) 038, arXiv:0709.1027 [hep-ph].
- [33] S. Höche et al., *QCD matrix elements and truncated showers*, **JHEP** **05** (2009) 053, arXiv:0903.1219 [hep-ph].
- [34] H.-L. Lai et al., *New parton distributions for collider physics*, **Phys. Rev.** **D82** (2010) 074024, arXiv:1007.2241 [hep-ph].
- [35] S. Agostinelli et al., *GEANT4 - a simulation toolkit*, **Nucl. Instrum. Methods A** **506** (2003) 250.
- [36] ATLAS Collaboration, *The ATLAS Simulation Infrastructure*, **Eur. Phys. J.** **C70** (2010) 823, arXiv:1005.4568 [physics.ins-det].
- [37] ATLAS Collaboration, *Summary of ATLAS Pythia 8 tunes*, ATL-PHYS-PUB-2012-003 (2012), URL: <https://cds.cern.ch/record/1474107>.
- [38] A. Martin et al., *Parton distributions for the LHC*, **Eur. Phys. J.** **C63** (2009) 189, arXiv:0901.0002 [hep-ph].
- [39] S. Catani et al., *Cross-section of isolated prompt photons in hadron hadron collisions*, **JHEP** **05** (2002) 028, arXiv:hep-ph/0204023.
- [40] L. Bourhis et al., *Next-to-leading order determination of fragmentation functions*, **Eur. Phys. J.** **C19** (2001) 89.
- [41] M. Cacciari and G. P. Salam, *Dispelling the N^3 myth for the k_t jet-finder*, **Phys. Lett.** **B641** (2006) 57, arXiv:hep-ph/0512210.
- [42] ATLAS Collaboration, *Electron and photon energy calibration with the ATLAS detector using LHC Run 1 data*, **Eur. Phys. J.** **C74** (2014) 3071, arXiv:1407.5063 [hep-ex].
- [43] M. Cacciari, G. P. Salam and G. Soyez, *The Catchment Area of Jets*, **JHEP** **04** (2008) 005.
- [44] M. Cacciari, G. P. Salam and S. Sapeta, *On the characterisation of the underlying event*, **JHEP** **04** (2010) 065.
- [45] ATLAS Collaboration, *Selection of jets produced in 13 TeV proton-proton collisions with the ATLAS detector*, ATLAS-CONF-2015-029 (2015), URL: <https://cds.cern.ch/record/2037702>.
- [46] ATLAS Collaboration, *Jet energy measurement and its systematic uncertainty in proton-proton collisions at $\sqrt{s} = 7$ TeV with the ATLAS detector*, **Eur. Phys. J.** **C75** (2015) 17, arXiv:1406.0076 [hep-ex].
- [47] ATLAS Collaboration, *Jet Calibration and Systematic Uncertainties for Jets Reconstructed in the ATLAS Detector at $\sqrt{s} = 13$ TeV*, ATL-PHYS-PUB-2015-015 (2015), URL: <https://cds.cern.ch/record/2037613>.

- [48] ATLAS Collaboration, *Performance of the ATLAS Electron and Photon Trigger in pp Collisions at $\sqrt{s} = 7$ TeV in 2011*, ATLAS-CONF-2012-048 (2012), URL: <https://cds.cern.ch/record/1450089>.
- [49] M. Rosenblatt, *Remarks on Some Nonparametric Estimates of a Density Function*, *Ann. Math. Statist.* **27** (Sept. 1956) 832.
- [50] E. Parzen, *On Estimation of a Probability Density Function and Mode*, *Ann. Math. Statist.* **33** (Sept. 1962) 1065.
- [51] M. Baak et al., *Interpolation between multi-dimensional histograms using a new non-linear moment morphing method*, *Nucl. Instrum. Methods A* **771** (2014) 39, arXiv:1410.7388 [physics.data-an].
- [52] R. M. Harris and K. Kousouris, *Searches for Dijet Resonances at Hadron Colliders*, *Int.J.Mod.Phys.* **A26** (2011) 5005, arXiv:1110.5302 [hep-ex].
- [53] ATLAS Collaboration, *Improved luminosity determination in pp collisions at $\sqrt{s} = 7$ TeV using the ATLAS detector at the LHC*, *Eur. Phys. J.* **C73** (2013) 2518, arXiv:1302.4393 [hep-ex].
- [54] G. Cowan et al., *Asymptotic formulae for likelihood-based tests of new physics*, *Eur. Phys. J.* **C71** (2011) 1554, [Erratum: *Eur. Phys. J.*C73 (2013) 2501], arXiv:1007.1727 [physics.data-an].
- [55] A. L. Read, *Presentation of search results: The CL_s technique*, *J. Phys. G: Nucl. Part. Phys* **28** (2002) 2693.

The ATLAS Collaboration

G. Aad⁸⁵, B. Abbott¹¹², J. Abdallah¹⁵⁰, O. Abdinov¹¹, B. Abeloos¹¹⁶, R. Aben¹⁰⁶, M. Abolins⁹⁰, O.S. AbouZeid¹³⁶, H. Abramowicz¹⁵², H. Abreu¹⁵¹, R. Abreu¹¹⁵, Y. Abulaiti^{145a,145b}, B.S. Acharya^{163a,163b,a}, L. Adamczyk^{38a}, D.L. Adams²⁵, J. Adelman¹⁰⁷, S. Adomeit⁹⁹, T. Adye¹³⁰, A.A. Affolder⁷⁴, T. Agatonovic-Jovin¹³, J. Agricola⁵⁴, J.A. Aguilar-Saavedra^{125a,125f}, S.P. Ahlen²², F. Ahmadov^{65,b}, G. Aielli^{132a,132b}, H. Akerstedt^{145a,145b}, T.P.A. Åkesson⁸¹, A.V. Akimov⁹⁵, G.L. Alberghi^{20a,20b}, J. Albert¹⁶⁸, S. Albrand⁵⁵, M.J. Alconada Verzini⁷¹, M. Aleksa³⁰, I.N. Aleksandrov⁶⁵, C. Alexa^{26b}, G. Alexander¹⁵², T. Alexopoulos¹⁰, M. Alhroob¹¹², G. Alimonti^{91a}, L. Alio⁸⁵, J. Alison³¹, S.P. Alkire³⁵, B.M.M. Allbrooke¹⁴⁸, B.W. Allen¹¹⁵, P.P. Allport¹⁸, A. Aloisio^{103a,103b}, A. Alonso³⁶, F. Alonso⁷¹, C. Alpigiani¹³⁷, B. Alvarez Gonzalez³⁰, D. Álvarez Piqueras¹⁶⁶, M.G. Alviggi^{103a,103b}, B.T. Amadio¹⁵, K. Amako⁶⁶, Y. Amaral Coutinho^{24a}, C. Amelung²³, D. Amidei⁸⁹, S.P. Amor Dos Santos^{125a,125c}, A. Amorim^{125a,125b}, S. Amoroso³⁰, N. Amram¹⁵², G. Amundsen²³, C. Anastopoulos¹³⁸, L.S. Ancu⁴⁹, N. Andari¹⁰⁷, T. Andeen³¹, C.F. Anders^{58b}, G. Anders³⁰, J.K. Anders⁷⁴, K.J. Anderson³¹, A. Andreazza^{91a,91b}, V. Andrei^{58a}, S. Angelidakis⁹, I. Angelozzi¹⁰⁶, P. Anger⁴⁴, A. Angerami³⁵, F. Anghinolfi³⁰, A.V. Anisenkov^{108,c}, N. Anjos¹², A. Annovi^{123a,123b}, M. Antonelli⁴⁷, A. Antonov⁹⁷, J. Antos^{143b}, F. Anulli^{131a}, M. Aoki⁶⁶, L. Aperio Bella¹⁸, G. Arabidze⁹⁰, Y. Arai⁶⁶, J.P. Araque^{125a}, A.T.H. Arce⁴⁵, F.A. Arduh⁷¹, J-F. Arguin⁹⁴, S. Argyropoulos⁶³, M. Arik^{19a}, A.J. Armbruster³⁰, L.J. Armitage⁷⁶, O. Arnaez³⁰, H. Arnold⁴⁸, M. Arratia²⁸, O. Arslan²¹, A. Artamonov⁹⁶, G. Artoni¹¹⁹, S. Artz⁸³, S. Asai¹⁵⁴, N. Asbah⁴², A. Ashkenazi¹⁵², B. Åsman^{145a,145b}, L. Asquith¹⁴⁸, K. Assamagan²⁵, R. Astalos^{143a}, M. Atkinson¹⁶⁴, N.B. Atlay¹⁴⁰, K. Augsten¹²⁷, G. Avolio³⁰, B. Axen¹⁵, M.K. Ayoub¹¹⁶, G. Azuelos^{94,d}, M.A. Baak³⁰, A.E. Baas^{58a}, M.J. Baca¹⁸, H. Bachacou¹³⁵, K. Bachas^{73a,73b}, M. Backes³⁰, M. Backhaus³⁰, P. Bagiacchi^{131a,131b}, P. Bagnaia^{131a,131b}, Y. Bai^{33a}, J.T. Baines¹³⁰, O.K. Baker¹⁷⁵, E.M. Baldin^{108,c}, P. Balek¹²⁸, T. Balestri¹⁴⁷, F. Balli¹³⁵, W.K. Balunas¹²¹, E. Banas³⁹, Sw. Banerjee^{172,e}, A.A.E. Bannoura¹⁷⁴, L. Barak³⁰, E.L. Barberio⁸⁸, D. Barberis^{50a,50b}, M. Barbero⁸⁵, T. Barillari¹⁰⁰, M. Barisonzi^{163a,163b}, T. Barklow¹⁴², N. Barlow²⁸, S.L. Barnes⁸⁴, B.M. Barnett¹³⁰, R.M. Barnett¹⁵, Z. Barnovska⁵, A. Baroncelli^{133a}, G. Barone²³, A.J. Barr¹¹⁹, L. Barranco Navarro¹⁶⁶, F. Barreiro⁸², J. Barreiro Guimarães da Costa^{33a}, R. Bartoldus¹⁴², A.E. Barton⁷², P. Bartos^{143a}, A. Basalae¹²², A. Bassalat¹¹⁶, A. Basye¹⁶⁴, R.L. Bates⁵³, S.J. Batista¹⁵⁷, J.R. Batley²⁸, M. Battaglia¹³⁶, M. Bauce^{131a,131b}, F. Bauer¹³⁵, H.S. Bawa^{142,f}, J.B. Beacham¹¹⁰, M.D. Beattie⁷², T. Beau⁸⁰, P.H. Beauchemin¹⁶⁰, R. Beccherle^{123a,123b}, P. Bechtel²¹, H.P. Beck^{17,g}, K. Becker¹¹⁹, M. Becker⁸³, M. Beckingham¹⁶⁹, C. Becot¹⁰⁹, A.J. Beddall^{19e}, A. Beddall^{19b}, V.A. Bednyakov⁶⁵, M. Bedognetti¹⁰⁶, C.P. Bee¹⁴⁷, L.J. Beemster¹⁰⁶, T.A. Beermann³⁰, M. Begel²⁵, J.K. Behr¹¹⁹, C. Belanger-Champagne⁸⁷, A.S. Bell⁷⁸, W.H. Bell⁴⁹, G. Bella¹⁵², L. Bellagamba^{20a}, A. Bellerive²⁹, M. Bellomo⁸⁶, K. Belotskiy⁹⁷, O. Beltramello³⁰, N.L. Belyaev⁹⁷, O. Benary¹⁵², D. Benchekroun^{134a}, M. Bender⁹⁹, K. Bendtz^{145a,145b}, N. Benekos¹⁰, Y. Benhammou¹⁵², E. Benhar Noccioli¹⁷⁵, J. Benitez⁶³, J.A. Benitez Garcia^{158b}, D.P. Benjamin⁴⁵, J.R. Bensinger²³, S. Bentvelsen¹⁰⁶, L. Beresford¹¹⁹, M. Beretta⁴⁷, D. Berge¹⁰⁶, E. Bergeas Kuutmann¹⁶⁵, N. Berger⁵, F. Berghaus¹⁶⁸, J. Beringer¹⁵, S. Berlendis⁵⁵, C. Bernard²², N.R. Bernard⁸⁶, C. Bernius¹⁰⁹, F.U. Bernlochner²¹, T. Berry⁷⁷, P. Berta¹²⁸, C. Bertella⁸³, G. Bertoli^{145a,145b}, F. Bertolucci^{123a,123b}, C. Bertsche¹¹², D. Bertsche¹¹², G.J. Besjes³⁶, O. Bessidskaia Bylund^{145a,145b}, M. Bessner⁴², N. Besson¹³⁵, C. Betancourt⁴⁸, S. Bethke¹⁰⁰, A.J. Bevan⁷⁶, W. Bhimji¹⁵, R.M. Bianchi¹²⁴, L. Bianchini²³, M. Bianco³⁰, O. Biebel⁹⁹, D. Biedermann¹⁶, R. Bielski⁸⁴, N.V. Biesuz^{123a,123b}, M. Biglietti^{133a}, J. Bilbao De Mendizabal⁴⁹, H. Bilokon⁴⁷, M. Bindi⁵⁴, S. Binet¹¹⁶, A. Bingul^{19b}, C. Bini^{131a,131b}, S. Biondi^{20a,20b}, D.M. Bjergaard⁴⁵, C.W. Black¹⁴⁹, J.E. Black¹⁴², K.M. Black²², D. Blackburn¹³⁷, R.E. Blair⁶, J.-B. Blanchard¹³⁵,

J.E. Blanco⁷⁷, T. Blazek^{143a}, I. Bloch⁴², C. Blocker²³, W. Blum^{83,*}, U. Blumenschein⁵⁴, S. Blunier^{32a}, G.J. Bobbink¹⁰⁶, V.S. Bobrovnikov^{108.c}, S.S. Bocchetta⁸¹, A. Bocci⁴⁵, C. Bock⁹⁹, M. Boehler⁴⁸, D. Boerner¹⁷⁴, J.A. Bogaerts³⁰, D. Bogavac¹³, A.G. Bogdanchikov¹⁰⁸, C. Bohm^{145a}, V. Boisvert⁷⁷, T. Bold^{38a}, V. Boldea^{26b}, A.S. Boldyrev⁹⁸, M. Bomben⁸⁰, M. Bona⁷⁶, M. Boonekamp¹³⁵, A. Borisov¹²⁹, G. Borissov⁷², J. Bortfeldt⁹⁹, D. Bortoletto¹¹⁹, V. Bortolotto^{60a,60b,60c}, K. Bos¹⁰⁶, D. Boscherini^{20a}, M. Bosman¹², J.D. Bossio Sola²⁷, J. Boudreau¹²⁴, J. Bouffard², E.V. Bouhova-Thacker⁷², D. Boumediene³⁴, C. Bourdarios¹¹⁶, N. Bousson¹¹³, S.K. Boutle⁵³, A. Boveia³⁰, J. Boyd³⁰, I.R. Boyko⁶⁵, J. Bracinik¹⁸, A. Brandt⁸, G. Brandt⁵⁴, O. Brandt^{58a}, U. Bratzler¹⁵⁵, B. Brau⁸⁶, J.E. Brau¹¹⁵, H.M. Braun^{174,*}, W.D. Breaden Madden⁵³, K. Brendlinger¹²¹, A.J. Brennan⁸⁸, L. Brenner¹⁰⁶, R. Brenner¹⁶⁵, S. Bressler¹⁷¹, T.M. Bristow⁴⁶, D. Britton⁵³, D. Britzger⁴², F.M. Brochu²⁸, I. Brock²¹, R. Brock⁹⁰, G. Brooijmans³⁵, T. Brooks⁷⁷, W.K. Brooks^{32b}, J. Brosamer¹⁵, E. Brost¹¹⁵, J.H. Broughton¹⁸, P.A. Bruckman de Renstrom³⁹, D. Bruncko^{143b}, R. Bruneliere⁴⁸, A. Bruni^{20a}, G. Bruni^{20a}, B.H. Brunt²⁸, M. Bruschi^{20a}, N. Bruscinò²¹, P. Bryant³¹, L. Bryngemark⁸¹, T. Buanes¹⁴, Q. Buat¹⁴¹, P. Buchholz¹⁴⁰, A.G. Buckley⁵³, I.A. Budagov⁶⁵, F. Buehrer⁴⁸, M.K. Bugge¹¹⁸, O. Bulekov⁹⁷, D. Bullock⁸, H. Burckhart³⁰, S. Burdin⁷⁴, C.D. Burgard⁴⁸, B. Burghgrave¹⁰⁷, K. Burka³⁹, S. Burke¹³⁰, I. Burmeister⁴³, E. Busato³⁴, D. Büscher⁴⁸, V. Büscher⁸³, P. Bussey⁵³, J.M. Butler²², A.I. Butt³, C.M. Buttar⁵³, J.M. Butterworth⁷⁸, P. Butti¹⁰⁶, W. Buttinger²⁵, A. Buzatu⁵³, A.R. Buzykaev^{108.c}, S. Cabrera Urbán¹⁶⁶, D. Caforio¹²⁷, V.M. Cairo^{37a,37b}, O. Cakir^{4a}, N. Calace⁴⁹, P. Calafiura¹⁵, A. Calandri⁸⁵, G. Calderini⁸⁰, P. Calfayan⁹⁹, L.P. Caloba^{24a}, D. Calvet³⁴, S. Calvet³⁴, T.P. Calvet⁸⁵, R. Camacho Toro³¹, S. Camarda⁴², P. Camarri^{132a,132b}, D. Cameron¹¹⁸, R. Caminal Armadans¹⁶⁴, C. Camincher⁵⁵, S. Campana³⁰, M. Campanelli⁷⁸, A. Campoverde¹⁴⁷, V. Canale^{103a,103b}, A. Canepa^{158a}, M. Cano Bret^{33e}, J. Cantero⁸², R. Cantrill^{125a}, T. Cao⁴⁰, M.D.M. Capeans Garrido³⁰, I. Caprini^{26b}, M. Caprini^{26b}, M. Capua^{37a,37b}, R. Caputo⁸³, R.M. Carbone³⁵, R. Cardarelli^{132a}, F. Cardillo⁴⁸, T. Carli³⁰, G. Carlino^{103a}, L. Carminati^{91a,91b}, S. Caron¹⁰⁵, E. Carquin^{32a}, G.D. Carrillo-Montoya³⁰, J.R. Carter²⁸, J. Carvalho^{125a,125c}, D. Casadei⁷⁸, M.P. Casado^{12,h}, M. Casolino¹², D.W. Casper¹⁶², E. Castaneda-Miranda^{144a}, A. Castelli¹⁰⁶, V. Castillo Gimenez¹⁶⁶, N.F. Castro^{125a,i}, A. Catinaccio³⁰, J.R. Catmore¹¹⁸, A. Cattai³⁰, J. Caudron⁸³, V. Cavaliere¹⁶⁴, D. Cavalli^{91a}, M. Cavalli-Sforza¹², V. Cavasinni^{123a,123b}, F. Ceradini^{133a,133b}, L. Cerda Alberich¹⁶⁶, B.C. Cerio⁴⁵, A.S. Cerqueira^{24b}, A. Cerri¹⁴⁸, L. Cerrito⁷⁶, F. Cerutti¹⁵, M. Cerv³⁰, A. Cervelli¹⁷, S.A. Cetin^{19d}, A. Chafaq^{134a}, D. Chakraborty¹⁰⁷, I. Chalupkova¹²⁸, Y.L. Chan^{60a}, P. Chang¹⁶⁴, J.D. Chapman²⁸, D.G. Charlton¹⁸, C.C. Chau¹⁵⁷, C.A. Chavez Barajas¹⁴⁸, S. Che¹¹⁰, S. Cheatham⁷², A. Chegwidan⁹⁰, S. Chekanov⁶, S.V. Chekulaev^{158a}, G.A. Chelkov^{65,j}, M.A. Chelstowska⁸⁹, C. Chen⁶⁴, H. Chen²⁵, K. Chen¹⁴⁷, S. Chen^{33c}, S. Chen¹⁵⁴, X. Chen^{33f}, Y. Chen⁶⁷, H.C. Cheng⁸⁹, Y. Cheng³¹, A. Cheplakov⁶⁵, E. Cheremushkina¹²⁹, R. Cherkaoui El Moursli^{134e}, V. Chernyatin^{25,*}, E. Cheu⁷, L. Chevalier¹³⁵, V. Chiarella⁴⁷, G. Chiarelli^{123a,123b}, G. Chiodini^{73a}, A.S. Chisholm¹⁸, A. Chitan^{26b}, M.V. Chizhov⁶⁵, K. Choi⁶¹, S. Chouridou⁹, B.K.B. Chow⁹⁹, V. Christodoulou⁷⁸, D. Chromek-Burckhart³⁰, J. Chudoba¹²⁶, A.J. Chuinard⁸⁷, J.J. Chwastowski³⁹, L. Chytka¹¹⁴, G. Ciapetti^{131a,131b}, A.K. Ciftci^{4a}, D. Cinca⁵³, V. Cindro⁷⁵, I.A. Cioara²¹, A. Ciocio¹⁵, F. Ciroto^{103a,103b}, Z.H. Citron¹⁷¹, M. Ciubancan^{26b}, A. Clark⁴⁹, B.L. Clark⁵⁷, P.J. Clark⁴⁶, R.N. Clarke¹⁵, C. Clement^{145a,145b}, Y. Coadou⁸⁵, M. Cobal^{163a,163c}, A. Coccaro⁴⁹, J. Cochran⁶⁴, L. Coffey²³, L. Colasurdo¹⁰⁵, B. Cole³⁵, S. Cole¹⁰⁷, A.P. Colijn¹⁰⁶, J. Collot⁵⁵, T. Colombo³⁰, G. Compostella¹⁰⁰, P. Conde Muiño^{125a,125b}, E. Coniavitis⁴⁸, S.H. Connell^{144b}, I.A. Connelly⁷⁷, V. Consorti⁴⁸, S. Constantinescu^{26b}, C. Conta^{120a,120b}, G. Conti³⁰, F. Conventi^{103a,k}, M. Cooke¹⁵, B.D. Cooper⁷⁸, A.M. Cooper-Sarkar¹¹⁹, T. Cornelissen¹⁷⁴, M. Corradi^{131a,131b}, F. Corriveau^{87,l}, A. Corso-Radu¹⁶², A. Cortes-Gonzalez¹², G. Cortiana¹⁰⁰, G. Costa^{91a}, M.J. Costa¹⁶⁶, D. Costanzo¹³⁸, G. Cottin²⁸, G. Cowan⁷⁷, B.E. Cox⁸⁴, K. Cranmer¹⁰⁹, S.J. Crawley⁵³, G. Cree²⁹, S. Crépe-Renaudin⁵⁵, F. Crescioli⁸⁰, W.A. Cribbs^{145a,145b}, M. Crispin Ortuzar¹¹⁹, M. Cristinziani²¹, V. Croft¹⁰⁵, G. Crosetti^{37a,37b},

T. Cuhadar Donszelmann¹³⁸, J. Cummings¹⁷⁵, M. Curatolo⁴⁷, J. Cúth⁸³, C. Cuthbert¹⁴⁹, H. Czirr¹⁴⁰, P. Czodrowski³, S. D'Auria⁵³, M. D'Onofrio⁷⁴, M.J. Da Cunha Sargedas De Sousa^{125a,125b}, C. Da Via⁸⁴, W. Dabrowski^{38a}, T. Dai⁸⁹, O. Dale¹⁴, F. Dallaire⁹⁴, C. Dallapiccola⁸⁶, M. Dam³⁶, J.R. Dandoy³¹, N.P. Dang⁴⁸, A.C. Daniells¹⁸, N.S. Dann⁸⁴, M. Danninger¹⁶⁷, M. Dano Hoffmann¹³⁵, V. Dao⁴⁸, G. Darbo^{50a}, S. Darmora⁸, J. Dassoulas³, A. Dattagupta⁶¹, W. Davey²¹, C. David¹⁶⁸, T. Davidek¹²⁸, M. Davies¹⁵², P. Davison⁷⁸, Y. Davygora^{58a}, E. Dawe⁸⁸, I. Dawson¹³⁸, R.K. Daya-Ishmukhametova⁸⁶, K. De⁸, R. de Asmundis^{103a}, A. De Benedetti¹¹², S. De Castro^{20a,20b}, S. De Cecco⁸⁰, N. De Groot¹⁰⁵, P. de Jong¹⁰⁶, H. De la Torre⁸², F. De Lorenzi⁶⁴, D. De Pedis^{131a}, A. De Salvo^{131a}, U. De Sanctis¹⁴⁸, A. De Santo¹⁴⁸, J.B. De Vivie De Regie¹¹⁶, W.J. Dearnaley⁷², R. Debbe²⁵, C. Debenedetti¹³⁶, D.V. Dedovich⁶⁵, I. Deigaard¹⁰⁶, J. Del Peso⁸², T. Del Prete^{123a,123b}, D. Delgove¹¹⁶, F. Deliot¹³⁵, C.M. Delitzsch⁴⁹, M. Deliyergiyev⁷⁵, A. Dell'Acqua³⁰, L. Dell'Asta²², M. Dell'Orso^{123a,123b}, M. Della Pietra^{103a,k}, D. della Volpe⁴⁹, M. Delmastro⁵, P.A. Delsart⁵⁵, C. Deluca¹⁰⁶, D.A. DeMarco¹⁵⁷, S. Demers¹⁷⁵, M. Demichev⁶⁵, A. Demilly⁸⁰, S.P. Denisov¹²⁹, D. Denysiuk¹³⁵, D. Derendarz³⁹, J.E. Derkaoui^{134d}, F. Derue⁸⁰, P. Dervan⁷⁴, K. Desch²¹, C. Deterre⁴², K. Dette⁴³, P.O. Deviveiros³⁰, A. Dewhurst¹³⁰, S. Dhaliwal²³, A. Di Ciaccio^{132a,132b}, L. Di Ciaccio⁵, W.K. Di Clemente¹²¹, A. Di Domenico^{131a,131b}, C. Di Donato^{131a,131b}, A. Di Girolamo³⁰, B. Di Girolamo³⁰, A. Di Mattia¹⁵¹, B. Di Micco^{133a,133b}, R. Di Nardo⁴⁷, A. Di Simone⁴⁸, R. Di Sipio¹⁵⁷, D. Di Valentino²⁹, C. Diaconu⁸⁵, M. Diamond¹⁵⁷, F.A. Dias⁴⁶, M.A. Diaz^{32a}, E.B. Diehl⁸⁹, J. Dietrich¹⁶, S. Diglio⁸⁵, A. Dimitrievska¹³, J. Dingfelder²¹, P. Dita^{26b}, S. Dita^{26b}, F. Dittus³⁰, F. Djama⁸⁵, T. Djobava^{51b}, J.I. Djuvsland^{58a}, M.A.B. do Vale^{24c}, D. Dobos³⁰, M. Dobre^{26b}, C. Doglioni⁸¹, T. Dohmae¹⁵⁴, J. Dolejsi¹²⁸, Z. Dolezal¹²⁸, B.A. Dolgoshein^{97,*}, M. Donadelli^{24d}, S. Donati^{123a,123b}, P. Dondero^{120a,120b}, J. Donini³⁴, J. Dopke¹³⁰, A. Doria^{103a}, M.T. Dova⁷¹, A.T. Doyle⁵³, E. Drechsler⁵⁴, M. Dris¹⁰, Y. Du^{33d}, J. Duarte-Camperderros¹⁵², E. Duchovni¹⁷¹, G. Duckeck⁹⁹, O.A. Ducu^{26b}, D. Duda¹⁰⁶, A. Dudarev³⁰, L. Dufflot¹¹⁶, L. Duguid⁷⁷, M. Dührssen³⁰, M. Dunford^{58a}, H. Duran Yildiz^{4a}, M. Düren⁵², A. Durglishvili^{51b}, D. Duschinger⁴⁴, B. Dutta⁴², M. Dyndal^{38a}, C. Eckardt⁴², K.M. Ecker¹⁰⁰, R.C. Edgar⁸⁹, W. Edson², N.C. Edwards⁴⁶, T. Eifert³⁰, G. Eigen¹⁴, K. Einsweiler¹⁵, T. Ekelof¹⁶⁵, M. El Kacimi^{134c}, V. Ellajosyula⁸⁵, M. Ellert¹⁶⁵, S. Elles⁵, F. Ellinghaus¹⁷⁴, A.A. Elliot¹⁶⁸, N. Ellis³⁰, J. Elmsheuser⁹⁹, M. Elsing³⁰, D. Emeliyanov¹³⁰, Y. Enari¹⁵⁴, O.C. Endner⁸³, M. Endo¹¹⁷, J.S. Ennis¹⁶⁹, J. Erdmann⁴³, A. Ereditato¹⁷, G. Ernis¹⁷⁴, J. Ernst², M. Ernst²⁵, S. Errede¹⁶⁴, E. Ertel⁸³, M. Escalier¹¹⁶, H. Esch⁴³, C. Escobar¹²⁴, B. Esposito⁴⁷, A.I. Etienne¹³⁵, E. Etzion¹⁵², H. Evans⁶¹, A. Ezhilov¹²², L. Fabbri^{20a,20b}, G. Facini³¹, R.M. Fakhruddinov¹²⁹, S. Falciano^{131a}, R.J. Falla⁷⁸, J. Faltova¹²⁸, Y. Fang^{33a}, M. Fanti^{91a,91b}, A. Farbin⁸, A. Farilla^{133a}, C. Farina¹²⁴, T. Farooque¹², S. Farrell¹⁵, S.M. Farrington¹⁶⁹, P. Farthouat³⁰, F. Fassi^{134e}, P. Fassnacht³⁰, D. Fassouliotis⁹, M. Fauci Giannelli⁷⁷, A. Favareto^{50a,50b}, L. Fayard¹¹⁶, O.L. Fedin^{122,m}, W. Fedorko¹⁶⁷, S. Feigl¹¹⁸, L. Felgioni⁸⁵, C. Feng^{33d}, E.J. Feng³⁰, H. Feng⁸⁹, A.B. Fenyuk¹²⁹, L. Feremenga⁸, P. Fernandez Martinez¹⁶⁶, S. Fernandez Perez¹², J. Ferrando⁵³, A. Ferrari¹⁶⁵, P. Ferrari¹⁰⁶, R. Ferrari^{120a}, D.E. Ferreira de Lima⁵³, A. Ferrer¹⁶⁶, D. Ferrere⁴⁹, C. Ferretti⁸⁹, A. Ferretto Parodi^{50a,50b}, F. Fiedler⁸³, A. Filipčič⁷⁵, M. Filipuzzi⁴², F. Filthaut¹⁰⁵, M. Fincke-Keeler¹⁶⁸, K.D. Finelli¹⁴⁹, M.C.N. Fiolhais^{125a,125c}, L. Fiorini¹⁶⁶, A. Firan⁴⁰, A. Fischer², C. Fischer¹², J. Fischer¹⁷⁴, W.C. Fisher⁹⁰, N. Flaschel⁴², I. Fleck¹⁴⁰, P. Fleischmann⁸⁹, G.T. Fletcher¹³⁸, G. Fletcher⁷⁶, R.R.M. Fletcher¹²¹, T. Flick¹⁷⁴, A. Floderus⁸¹, L.R. Flores Castillo^{60a}, M.J. Flowerdew¹⁰⁰, G.T. Forcolin⁸⁴, A. Formica¹³⁵, A. Forti⁸⁴, D. Fournier¹¹⁶, H. Fox⁷², S. Fracchia¹², P. Francavilla⁸⁰, M. Franchini^{20a,20b}, D. Francis³⁰, L. Franconi¹¹⁸, M. Franklin⁵⁷, M. Frate¹⁶², M. Fraternali^{120a,120b}, D. Freeborn⁷⁸, S.M. Fressard-Batraneanu³⁰, F. Friedrich⁴⁴, D. Froidevaux³⁰, J.A. Frost¹¹⁹, C. Fukunaga¹⁵⁵, E. Fullana Torregrosa⁸³, T. Fusayasu¹⁰¹, J. Fuster¹⁶⁶, C. Gabaldon⁵⁵, O. Gabizon¹⁷⁴, A. Gabrielli^{20a,20b}, A. Gabrielli¹⁵, G.P. Gach^{38a}, S. Gadatsch³⁰, S. Gadomski⁴⁹, G. Gagliardi^{50a,50b}, P. Gagnon⁶¹, C. Galea¹⁰⁵, B. Galhardo^{125a,125c}, E.J. Gallas¹¹⁹, B.J. Gallop¹³⁰, P. Gallus¹²⁷, G. Galster³⁶, K.K. Gan¹¹⁰, J. Gao^{33b,85}, Y. Gao⁴⁶, Y.S. Gao^{142,f}, F.M. Garay Walls⁴⁶, C. García¹⁶⁶,

J.E. García Navarro¹⁶⁶, M. Garcia-Sciveres¹⁵, R.W. Gardner³¹, N. Garelli¹⁴², V. Garonne¹¹⁸,
 A. Gascon Bravo⁴², C. Gatti⁴⁷, A. Gaudiello^{50a,50b}, G. Gaudio^{120a}, B. Gaur¹⁴⁰, L. Gauthier⁹⁴,
 I.L. Gavrilenko⁹⁵, C. Gay¹⁶⁷, G. Gaycken²¹, E.N. Gazis¹⁰, Z. Gecse¹⁶⁷, C.N.P. Gee¹³⁰,
 Ch. Geich-Gimbel²¹, M.P. Geisler^{58a}, C. Gemme^{50a}, M.H. Genest⁵⁵, C. Geng^{33b,n}, S. Gentile^{131a,131b},
 S. George⁷⁷, D. Gerbaudo¹⁶², A. Gershon¹⁵², S. Ghasemi¹⁴⁰, H. Ghazlane^{134b}, B. Giacobbe^{20a},
 S. Giagu^{131a,131b}, P. Giannetti^{123a,123b}, B. Gibbard²⁵, S.M. Gibson⁷⁷, M. Gignac¹⁶⁷, M. Gilchriese¹⁵,
 T.P.S. Gillam²⁸, D. Gillberg²⁹, G. Gilles¹⁷⁴, D.M. Gingrich^{3,d}, N. Giokaris⁹, M.P. Giordani^{163a,163c},
 F.M. Giorgi^{20a}, F.M. Giorgi¹⁶, P.F. Giraud¹³⁵, P. Giromini⁵⁷, D. Giugni^{91a}, C. Giuliani¹⁰⁰, M. Giulini^{58b},
 B.K. Gjelsten¹¹⁸, S. Gkaitatzis¹⁵³, I. Gkialas¹⁵³, E.L. Gkoukousis¹¹⁶, L.K. Gladilin⁹⁸, C. Glasman⁸²,
 J. Glatzer³⁰, P.C.F. Glaysheer⁴⁶, A. Glazov⁴², M. Goblirsch-Kolb¹⁰⁰, J. Godlewski³⁹, S. Goldfarb⁸⁹,
 T. Golling⁴⁹, D. Golubkov¹²⁹, A. Gomes^{125a,125b,125d}, R. Gonçalo^{125a},
 J. Goncalves Pinto Firmino Da Costa¹³⁵, L. Gonella¹⁸, A. Gongadze⁶⁵, S. González de la Hoz¹⁶⁶,
 G. Gonzalez Parra¹², S. Gonzalez-Sevilla⁴⁹, L. Goossens³⁰, P.A. Gorbounov⁹⁶, H.A. Gordon²⁵,
 I. Gorelov¹⁰⁴, B. Gorini³⁰, E. Gorini^{73a,73b}, A. Gorišek⁷⁵, E. Gornicki³⁹, A.T. Goshaw⁴⁵, C. Gössling⁴³,
 M.I. Gostkin⁶⁵, C.R. Goudet¹¹⁶, D. Goujdami^{134c}, A.G. Goussiou¹³⁷, N. Govender^{144b}, E. Gozani¹⁵¹,
 L. Graber⁵⁴, I. Grabowska-Bold^{38a}, P.O.J. Gradin¹⁶⁵, P. Grafström^{20a,20b}, J. Gramling⁴⁹, E. Gramstad¹¹⁸,
 S. Grancagnolo¹⁶, V. Gratchev¹²², H.M. Gray³⁰, E. Graziani^{133a}, Z.D. Greenwood^{79,o}, C. Greife²¹,
 K. Gregersen⁷⁸, I.M. Gregor⁴², P. Grenier¹⁴², K. Grevtsov⁵, J. Griffiths⁸, A.A. Grillo¹³⁶, K. Grimm⁷²,
 S. Grinstein^{12,p}, Ph. Gris³⁴, J.-F. Grivaz¹¹⁶, S. Groh⁸³, J.P. Grohs⁴⁴, E. Gross¹⁷¹, J. Grosse-Knetter⁵⁴,
 G.C. Grossi⁷⁹, Z.J. Grout¹⁴⁸, L. Guan⁸⁹, W. Guan¹⁷², J. Guenther¹²⁷, F. Guescini⁴⁹, D. Guest¹⁶²,
 O. Gueta¹⁵², E. Guido^{50a,50b}, T. Guillemin⁵, S. Guindon², U. Gul⁵³, C. Gumpert³⁰, J. Guo^{33e},
 Y. Guo^{33b,n}, S. Gupta¹¹⁹, G. Gustavino^{131a,131b}, P. Gutierrez¹¹², N.G. Gutierrez Ortiz⁷⁸, C. Gutschow⁴⁴,
 C. Guyot¹³⁵, C. Gwenlan¹¹⁹, C.B. Gwilliam⁷⁴, A. Haas¹⁰⁹, C. Haber¹⁵, H.K. Hadavand⁸, N. Haddad^{134e},
 A. Hader⁸⁵, P. Haefner²¹, S. Hageböck²¹, Z. Hajduk³⁹, H. Hakobyan^{176,*}, M. Haleem⁴², J. Haley¹¹³,
 D. Hall¹¹⁹, G. Halladjian⁹⁰, G.D. Hallowell⁸⁵, K. Hamacher¹⁷⁴, P. Hamal¹¹⁴, K. Hamano¹⁶⁸,
 A. Hamilton^{144a}, G.N. Hamity¹³⁸, P.G. Hamnett⁴², L. Han^{33b}, K. Hanagaki^{66,q}, K. Hanawa¹⁵⁴,
 M. Hance¹³⁶, B. Haney¹²¹, P. Hanke^{58a}, R. Hanna¹³⁵, J.B. Hansen³⁶, J.D. Hansen³⁶, M.C. Hansen²¹,
 P.H. Hansen³⁶, K. Hara¹⁵⁹, A.S. Hard¹⁷², T. Harenberg¹⁷⁴, F. Hariri¹¹⁶, S. Harkusha⁹²,
 R.D. Harrington⁴⁶, P.F. Harrison¹⁶⁹, F. Hartjes¹⁰⁶, M. Hasegawa⁶⁷, Y. Hasegawa¹³⁹, A. Hasib¹¹²,
 S. Hassani¹³⁵, S. Haug¹⁷, R. Hauser⁹⁰, L. Hauswald⁴⁴, M. Havranek¹²⁶, C.M. Hawkes¹⁸,
 R.J. Hawkings³⁰, A.D. Hawkins⁸¹, D. Hayden⁹⁰, C.P. Hays¹¹⁹, J.M. Hays⁷⁶, H.S. Hayward⁷⁴,
 S.J. Haywood¹³⁰, S.J. Head¹⁸, T. Heck⁸³, V. Hedberg⁸¹, L. Heelan⁸, S. Heim¹²¹, T. Heim¹⁵,
 B. Heinemann¹⁵, J.J. Heinrich⁹⁹, L. Heinrich¹⁰⁹, C. Heinz⁵², J. Hejbal¹²⁶, L. Helary²²,
 S. Hellman^{145a,145b}, C. Helsen³⁰, J. Henderson¹¹⁹, R.C.W. Henderson⁷², Y. Heng¹⁷², S. Henkelmann¹⁶⁷,
 A.M. Henriques Correia³⁰, S. Henrot-Versille¹¹⁶, G.H. Herbert¹⁶, Y. Hernández Jiménez¹⁶⁶, G. Herten⁴⁸,
 R. Hertenberger⁹⁹, L. Hervas³⁰, G.G. Hesketh⁷⁸, N.P. Hessey¹⁰⁶, J.W. Hetherly⁴⁰, R. Hickling⁷⁶,
 E. Higón-Rodríguez¹⁶⁶, E. Hill¹⁶⁸, J.C. Hill²⁸, K.H. Hiller⁴², S.J. Hillier¹⁸, I. Hinchliffe¹⁵, E. Hines¹²¹,
 R.R. Hinman¹⁵, M. Hirose¹⁵⁶, D. Hirschbuehl¹⁷⁴, J. Hobbs¹⁴⁷, N. Hod¹⁰⁶, M.C. Hodgkinson¹³⁸,
 P. Hodgson¹³⁸, A. Hoecker³⁰, M.R. Hoferkamp¹⁰⁴, F. Hoenig⁹⁹, M. Hohlfeld⁸³, D. Hohn²¹,
 T.R. Holmes¹⁵, M. Homann⁴³, T.M. Hong¹²⁴, B.H. Hooberman¹⁶⁴, W.H. Hopkins¹¹⁵, Y. Horii¹⁰²,
 A.J. Horton¹⁴¹, J.-Y. Hostachy⁵⁵, S. Hou¹⁵⁰, A. Hoummada^{134a}, J. Howard¹¹⁹, J. Howarth⁴²,
 M. Hrabovsky¹¹⁴, I. Hristova¹⁶, J. Hrivnac¹¹⁶, T. Hryn'ova⁵, A. Hrynevich⁹³, C. Hsu^{144c}, P.J. Hsu^{150,r},
 S.-C. Hsu¹³⁷, D. Hu³⁵, Q. Hu^{33b}, Y. Huang⁴², Z. Hubacek¹²⁷, F. Hubaut⁸⁵, F. Huegging²¹,
 T.B. Huffman¹¹⁹, E.W. Hughes³⁵, G. Hughes⁷², M. Huhtinen³⁰, T.A. Hülsing⁸³, N. Huseynov^{65,b},
 J. Huston⁹⁰, J. Huth⁵⁷, G. Iacobucci⁴⁹, G. Iakovidis²⁵, I. Ibragimov¹⁴⁰, L. Iconomidou-Fayard¹¹⁶,
 E. Ideal¹⁷⁵, Z. Idrissi^{134e}, P. Iengo³⁰, O. Igonkina¹⁰⁶, T. Iizawa¹⁷⁰, Y. Ikegami⁶⁶, M. Ikeno⁶⁶,
 Y. Ilchenko^{31,s}, D. Iliadis¹⁵³, N. Ilic¹⁴², T. Ince¹⁰⁰, G. Introzzi^{120a,120b}, P. Ioannou⁹, M. Iodice^{133a},

K. Iordanidou³⁵, V. Ippolito⁵⁷, A. Irlles Quiles¹⁶⁶, C. Isaksson¹⁶⁵, M. Ishino⁶⁸, M. Ishitsuka¹⁵⁶,
 R. Ishmukhametov¹¹⁰, C. Issever¹¹⁹, S. Istin^{19a}, F. Ito¹⁵⁹, J.M. Iturbe Ponce⁸⁴, R. Iuppa^{132a,132b},
 J. Ivarsson⁸¹, W. Iwanski³⁹, H. Iwasaki⁶⁶, J.M. Izen⁴¹, V. Izzo^{103a}, S. Jabbar³, B. Jackson¹²¹,
 M. Jackson⁷⁴, P. Jackson¹, V. Jain², K.B. Jakobi⁸³, K. Jakobs⁴⁸, S. Jakobsen³⁰, T. Jakoubek¹²⁶,
 D.O. Jamin¹¹³, D.K. Jana⁷⁹, E. Jansen⁷⁸, R. Jansky⁶², J. Janssen²¹, M. Janus⁵⁴, G. Jarlskog⁸¹,
 N. Javadov^{65,b}, T. Javůrek⁴⁸, F. Jeanneau¹³⁵, L. Jeanty¹⁵, J. Jejelava^{51a,t}, G.-Y. Jeng¹⁴⁹, D. Jennens⁸⁸,
 P. Jenni^{48,u}, J. Jentzsch⁴³, C. Jeske¹⁶⁹, S. Jézéquel⁵, H. Ji¹⁷², J. Jia¹⁴⁷, H. Jiang⁶⁴, Y. Jiang^{33b},
 S. Jiggins⁷⁸, J. Jimenez Pena¹⁶⁶, S. Jin^{33a}, A. Jinaru^{26b}, O. Jinnouchi¹⁵⁶, P. Johansson¹³⁸, K.A. Johns⁷,
 W.J. Johnson¹³⁷, K. Jon-And^{145a,145b}, G. Jones¹⁶⁹, R.W.L. Jones⁷², S. Jones⁷, T.J. Jones⁷⁴,
 J. Jongmanns^{58a}, P.M. Jorge^{125a,125b}, J. Jovicevic^{158a}, X. Ju¹⁷², A. Juste Rozas^{12,p}, M.K. Köhler¹⁷¹,
 M. Kaci¹⁶⁶, A. Kaczmarek³⁹, M. Kado¹¹⁶, H. Kagan¹¹⁰, M. Kagan¹⁴², S.J. Kahn⁸⁵, E. Kajomovitz⁴⁵,
 C.W. Kalderon¹¹⁹, A. Kaluza⁸³, S. Kama⁴⁰, A. Kamenshchikov¹²⁹, N. Kanaya¹⁵⁴, S. Kaneti²⁸,
 V.A. Kantserov⁹⁷, J. Kanzaki⁶⁶, B. Kaplan¹⁰⁹, L.S. Kaplan¹⁷², A. Kapliy³¹, D. Kar^{144c}, K. Karakostas¹⁰,
 A. Karamaoun³, N. Karastathis^{10,106}, M.J. Kareem⁵⁴, E. Karentzos¹⁰, M. Karnevskiy⁸³, S.N. Karpov⁶⁵,
 Z.M. Karpova⁶⁵, K. Karthik¹⁰⁹, V. Kartvelishvili⁷², A.N. Karyukhin¹²⁹, K. Kasahara¹⁵⁹, L. Kashif⁷²,
 R.D. Kass¹¹⁰, A. Kastanas¹⁴, Y. Kataoka¹⁵⁴, C. Kato¹⁵⁴, A. Katre⁴⁹, J. Katzy⁴², K. Kawade¹⁰²,
 K. Kawagoe⁷⁰, T. Kawamoto¹⁵⁴, G. Kawamura⁵⁴, S. Kazama¹⁵⁴, V.F. Kazanin^{108,c}, R. Keeler¹⁶⁸,
 R. Kehoe⁴⁰, J.S. Keller⁴², J.J. Kempster⁷⁷, H. Keoshkerian⁸⁴, O. Kepka¹²⁶, B.P. Kerševan⁷⁵,
 S. Kersten¹⁷⁴, R.A. Keyes⁸⁷, F. Khalil-zada¹¹, H. Khandanyan^{145a,145b}, A. Khanov¹¹³,
 A.G. Kharlamov^{108,c}, T.J. Khoo²⁸, V. Khovanskij⁹⁶, E. Khramov⁶⁵, J. Khubua^{51b,v}, S. Kido⁶⁷,
 H.Y. Kim⁸, S.H. Kim¹⁵⁹, Y.K. Kim³¹, N. Kimura¹⁵³, O.M. Kind¹⁶, B.T. King⁷⁴, M. King¹⁶⁶,
 S.B. King¹⁶⁷, J. Kirk¹³⁰, A.E. Kiryunin¹⁰⁰, T. Kishimoto⁶⁷, D. Kisielewska^{38a}, F. Kiss⁴⁸, K. Kiuchi¹⁵⁹,
 O. Kivernyk¹³⁵, E. Kladiva^{143b}, M.H. Klein³⁵, M. Klein⁷⁴, U. Klein⁷⁴, K. Kleinknecht⁸³,
 P. Klimek^{145a,145b}, A. Klimentov²⁵, R. Klingenberg⁴³, J.A. Klinger¹³⁸, T. Klioutchnikova³⁰,
 E.-E. Kluge^{58a}, P. Kluit¹⁰⁶, S. Kluth¹⁰⁰, J. Knapik³⁹, E. Kneringer⁶², E.B.F.G. Knoops⁸⁵, A. Knue⁵³,
 A. Kobayashi¹⁵⁴, D. Kobayashi¹⁵⁶, T. Kobayashi¹⁵⁴, M. Kobel⁴⁴, M. Kocian¹⁴², P. Kodys¹²⁸, T. Koffas²⁹,
 E. Koffeman¹⁰⁶, L.A. Kogan¹¹⁹, T. Kohriki⁶⁶, T. Koi¹⁴², H. Kolanoski¹⁶, M. Kolb^{58b}, I. Koletsou⁵,
 A.A. Komar^{95,*}, Y. Komori¹⁵⁴, T. Kondo⁶⁶, N. Kondrashova⁴², K. Köneke⁴⁸, A.C. König¹⁰⁵,
 T. Kono^{66,w}, R. Konoplich^{109,x}, N. Konstantinidis⁷⁸, R. Kopeliansky⁶¹, S. Koperny^{38a}, L. Köpke⁸³,
 A.K. Kopp⁴⁸, K. Korcyl³⁹, K. Kordas¹⁵³, A. Korn⁷⁸, A.A. Korol^{108,c}, I. Korolkov¹², E.V. Korolkova¹³⁸,
 O. Kortner¹⁰⁰, S. Kortner¹⁰⁰, T. Kosek¹²⁸, V.V. Kostyukhin²¹, V.M. Kotov⁶⁵, A. Kotwal⁴⁵,
 A. Kourkoumeli-Charalampidi¹⁵³, C. Kourkoumelis⁹, V. Kouskoura²⁵, A. Koutsman^{158a},
 R. Kowalewski¹⁶⁸, T.Z. Kowalski^{38a}, W. Kozanecki¹³⁵, A.S. Kozhin¹²⁹, V.A. Kramarenko⁹⁸,
 G. Kramberger⁷⁵, D. Krasnopevtsev⁹⁷, M.W. Krasny⁸⁰, A. Krasznahorkay³⁰, J.K. Kraus²¹,
 A. Kravchenko²⁵, M. Kretz^{58c}, J. Kretzschmar⁷⁴, K. Kreutzfeldt⁵², P. Krieger¹⁵⁷, K. Krizka³¹,
 K. Kroeninger⁴³, H. Kroha¹⁰⁰, J. Kroll¹²¹, J. Kroseberg²¹, J. Krstic¹³, U. Kruchonak⁶⁵, H. Krüger²¹,
 N. Krumnack⁶⁴, A. Kruse¹⁷², M.C. Kruse⁴⁵, M. Kruskal²², T. Kubota⁸⁸, H. Kucuk⁷⁸, S. Kудay^{4b},
 J.T. Kuechler¹⁷⁴, S. Kuehn⁴⁸, A. Kugel^{58c}, F. Kuger¹⁷³, A. Kuhl¹³⁶, T. Kuhl⁴², V. Kukhtin⁶⁵,
 R. Kukla¹³⁵, Y. Kulchitsky⁹², S. Kuleshov^{32b}, M. Kuna^{131a,131b}, T. Kunigo⁶⁸, A. Kupco¹²⁶,
 H. Kurashige⁶⁷, Y.A. Kurochkin⁹², V. Kus¹²⁶, E.S. Kuwertz¹⁶⁸, M. Kuze¹⁵⁶, J. Kvita¹¹⁴, T. Kwan¹⁶⁸,
 D. Kyriazopoulos¹³⁸, A. La Rosa¹⁰⁰, J.L. La Rosa Navarro^{24d}, L. La Rotonda^{37a,37b}, C. Lacasta¹⁶⁶,
 F. Lacava^{131a,131b}, J. Lacey²⁹, H. Lacker¹⁶, D. Lacour⁸⁰, V.R. Lacuesta¹⁶⁶, E. Ladygin⁶⁵, R. Lafaye⁵,
 B. Laforge⁸⁰, T. Lagouri¹⁷⁵, S. Lai⁵⁴, S. Lammers⁶¹, W. Lampl⁷, E. Lançon¹³⁵, U. Landgraf⁴⁸,
 M.P.J. Landon⁷⁶, V.S. Lang^{58a}, J.C. Lange¹², A.J. Lankford¹⁶², F. Lanni²⁵, K. Lantzscht²¹, A. Lanza^{120a},
 S. Laplace⁸⁰, C. Lapoire³⁰, J.F. Laporte¹³⁵, T. Lari^{91a}, F. Lasagni Manghi^{20a,20b}, M. Lassnig³⁰,
 P. Laurelli⁴⁷, W. Lavrijsen¹⁵, A.T. Law¹³⁶, P. Laycock⁷⁴, T. Lazovich⁵⁷, O. Le Dortz⁸⁰, E. Le Guirriec⁸⁵,
 E. Le Menedeu¹², E.P. Le Quilleuc¹³⁵, M. LeBlanc¹⁶⁸, T. LeCompte⁶, F. Ledroit-Guillon⁵⁵, C.A. Lee²⁵,

S.C. Lee¹⁵⁰, L. Lee¹, G. Lefebvre⁸⁰, M. Lefebvre¹⁶⁸, F. Legger⁹⁹, C. Leggett¹⁵, A. Lehan⁷⁴, G. Lehmann Miotto³⁰, X. Lei⁷, W.A. Leight²⁹, A. Leisos^{153,y}, A.G. Leister¹⁷⁵, M.A.L. Leite^{24d}, R. Leitner¹²⁸, D. Lellouch¹⁷¹, B. Lemmer⁵⁴, K.J.C. Leney⁷⁸, T. Lenz²¹, B. Lenzi³⁰, R. Leone⁷, S. Leone^{123a,123b}, C. Leonidopoulos⁴⁶, S. Leontsinis¹⁰, C. Leroy⁹⁴, A.A.J. Lesage¹³⁵, C.G. Lester²⁸, M. Levchenko¹²², J. Levêque⁵, D. Levin⁸⁹, L.J. Levinson¹⁷¹, M. Levy¹⁸, A.M. Leyko²¹, M. Leyton⁴¹, B. Li^{33b,z}, H. Li¹⁴⁷, H.L. Li³¹, L. Li⁴⁵, L. Li^{33e}, Q. Li^{33a}, S. Li⁴⁵, X. Li⁸⁴, Y. Li¹⁴⁰, Z. Liang¹³⁶, H. Liao³⁴, B. Liberti^{132a}, A. Liblong¹⁵⁷, P. Lichard³⁰, K. Lie¹⁶⁴, J. Liebal²¹, W. Liebig¹⁴, C. Limbach²¹, A. Limosani¹⁴⁹, S.C. Lin^{150,aa}, T.H. Lin⁸³, B.E. Lindquist¹⁴⁷, E. Lipeles¹²¹, A. Lipniacka¹⁴, M. Lisovyi^{58b}, T.M. Liss¹⁶⁴, D. Lissauer²⁵, A. Lister¹⁶⁷, A.M. Litke¹³⁶, B. Liu^{150,ab}, D. Liu¹⁵⁰, H. Liu⁸⁹, H. Liu²⁵, J. Liu⁸⁵, J.B. Liu^{33b}, K. Liu⁸⁵, L. Liu¹⁶⁴, M. Liu⁴⁵, M. Liu^{33b}, Y.L. Liu^{33b}, Y. Liu^{33b}, M. Livan^{120a,120b}, A. Lleres⁵⁵, J. Llorente Merino⁸², S.L. Lloyd⁷⁶, F. Lo Sterzo¹⁵⁰, E. Lobodzinska⁴², P. Loch⁷, W.S. Lockman¹³⁶, F.K. Loebinger⁸⁴, A.E. Loevschall-Jensen³⁶, K.M. Loew²³, A. Loginov¹⁷⁵, T. Lohse¹⁶, K. Lohwasser⁴², M. Lokajicek¹²⁶, B.A. Long²², J.D. Long¹⁶⁴, R.E. Long⁷², L. Longo^{73a,73b}, K.A. Looper¹¹⁰, L. Lopes^{125a}, D. Lopez Mateos⁵⁷, B. Lopez Paredes¹³⁸, I. Lopez Paz¹², A. Lopez Solis⁸⁰, J. Lorenz⁹⁹, N. Lorenzo Martinez⁶¹, M. Losada¹⁶¹, P.J. Lösel⁹⁹, X. Lou^{33a}, A. Lounis¹¹⁶, J. Love⁶, P.A. Love⁷², H. Lu^{60a}, N. Lu⁸⁹, H.J. Lubatti¹³⁷, C. Luci^{131a,131b}, A. Lucotte⁵⁵, C. Luedtke⁴⁸, F. Luehring⁶¹, W. Lukas⁶², L. Luminari^{131a}, O. Lundberg^{145a,145b}, B. Lund-Jensen¹⁴⁶, D. Lynn²⁵, R. Lysak¹²⁶, E. Lytken⁸¹, H. Ma²⁵, L.L. Ma^{33d}, G. Maccarrone⁴⁷, A. Macchiolo¹⁰⁰, C.M. Macdonald¹³⁸, B. Maček⁷⁵, J. Machado Miguens^{121,125b}, D. Madaffari⁸⁵, R. Madar³⁴, H.J. Maddocks¹⁶⁵, W.F. Mader⁴⁴, A. Madsen⁴², J. Maeda⁶⁷, S. Maeland¹⁴, T. Maeno²⁵, A. Maevskiy⁹⁸, E. Magradze⁵⁴, J. Mahlstedt¹⁰⁶, C. Maiani¹¹⁶, C. Maidantchik^{24a}, A.A. Maier¹⁰⁰, T. Maier⁹⁹, A. Maio^{125a,125b,125d}, S. Majewski¹¹⁵, Y. Makida⁶⁶, N. Makovec¹¹⁶, B. Malaescu⁸⁰, Pa. Malecki³⁹, V.P. Maleev¹²², F. Malek⁵⁵, U. Mallik⁶³, D. Malon⁶, C. Malone¹⁴², S. Maltezos¹⁰, V.M. Malyshev¹⁰⁸, S. Malyukov³⁰, J. Mamuzic⁴², G. Mancini⁴⁷, B. Mandelli³⁰, L. Mandelli^{91a}, I. Mandić⁷⁵, J. Maneira^{125a,125b}, L. Manhaes de Andrade Filho^{24b}, J. Manjarres Ramos^{158b}, A. Mann⁹⁹, B. Mansoulie¹³⁵, R. Mantifel⁸⁷, M. Mantoani⁵⁴, S. Manzoni^{91a,91b}, L. Mapelli³⁰, G. Marceca²⁷, L. March⁴⁹, G. Marchiori⁸⁰, M. Marcisovsky¹²⁶, M. Marjanovic¹³, D.E. Marley⁸⁹, F. Marroquim^{24a}, S.P. Marsden⁸⁴, Z. Marshall¹⁵, L.F. Marti¹⁷, S. Marti-Garcia¹⁶⁶, B. Martin⁹⁰, T.A. Martin¹⁶⁹, V.J. Martin⁴⁶, B. Martin dit Latour¹⁴, M. Martinez^{12,p}, S. Martin-Haugh¹³⁰, V.S. Martoiu^{26b}, A.C. Martyniuk⁷⁸, M. Marx¹³⁷, F. Marzano^{131a}, A. Marzin³⁰, L. Masetti⁸³, T. Mashimo¹⁵⁴, R. Mashinistov⁹⁵, J. Masik⁸⁴, A.L. Maslennikov^{108,c}, I. Massa^{20a,20b}, L. Massa^{20a,20b}, P. Mastrandrea⁵, A. Mastroberardino^{37a,37b}, T. Masubuchi¹⁵⁴, P. Mättig¹⁷⁴, J. Mattmann⁸³, J. Maurer^{26b}, S.J. Maxfield⁷⁴, D.A. Maximov^{108,c}, R. Mazini¹⁵⁰, S.M. Mazza^{91a,91b}, N.C. Mc Fadden¹⁰⁴, G. Mc Goldrick¹⁵⁷, S.P. Mc Kee⁸⁹, A. McCarn⁸⁹, R.L. McCarthy¹⁴⁷, T.G. McCarthy²⁹, L.I. McClymont⁷⁸, K.W. McFarlane^{56,*}, J.A. Mcfayden⁷⁸, G. Mchedlidze⁵⁴, S.J. McMahon¹³⁰, R.A. McPherson^{168,l}, M. Medinnis⁴², S. Meehan¹³⁷, S. Mehlhase⁹⁹, A. Mehta⁷⁴, K. Meier^{58a}, C. Meineck⁹⁹, B. Meirose⁴¹, B.R. Mellado Garcia^{144c}, F. Meloni¹⁷, A. Mengarelli^{20a,20b}, S. Menke¹⁰⁰, E. Meoni¹⁶⁰, K.M. Mercurio⁵⁷, S. Mergelmeyer¹⁶, P. Mermod⁴⁹, L. Merola^{103a,103b}, C. Meroni^{91a}, F.S. Merritt³¹, A. Messina^{131a,131b}, J. Metcalfe⁶, A.S. Mete¹⁶², C. Meyer⁸³, C. Meyer¹²¹, J-P. Meyer¹³⁵, J. Meyer¹⁰⁶, H. Meyer Zu Theenhausen^{58a}, R.P. Middleton¹³⁰, S. Miglioranza^{163a,163c}, L. Mijović²¹, G. Mikenberg¹⁷¹, M. Mikestikova¹²⁶, M. Mikuz⁷⁵, M. Milesi⁸⁸, A. Milic³⁰, D.W. Miller³¹, C. Mills⁴⁶, A. Milov¹⁷¹, D.A. Milstead^{145a,145b}, A.A. Minaenko¹²⁹, Y. Minami¹⁵⁴, I.A. Minashvili⁶⁵, A.I. Mincer¹⁰⁹, B. Mindur^{38a}, M. Mineev⁶⁵, Y. Ming¹⁷², L.M. Mir¹², K.P. Mistry¹²¹, T. Mitani¹⁷⁰, J. Mitrevski⁹⁹, V.A. Mitsou¹⁶⁶, A. Miucci⁴⁹, P.S. Miyagawa¹³⁸, J.U. Mjörnmark⁸¹, T. Moa^{145a,145b}, K. Mochizuki⁸⁵, S. Mohapatra³⁵, W. Mohr⁴⁸, S. Molander^{145a,145b}, R. Moles-Valls²¹, R. Monden⁶⁸, M.C. Mondragon⁹⁰, K. Mönig⁴², J. Monk³⁶, E. Monnier⁸⁵, A. Montalbano¹⁴⁷, J. Montejo Berlingen³⁰, F. Monticelli⁷¹, S. Monzani^{91a,91b}, R.W. Moore³, N. Morange¹¹⁶, D. Moreno¹⁶¹, M. Moreno Llácer⁵⁴, P. Morettini^{50a},

D. Mori¹⁴¹, T. Mori¹⁵⁴, M. Morii⁵⁷, M. Morinaga¹⁵⁴, V. Morisbak¹¹⁸, S. Moritz⁸³, A.K. Morley¹⁴⁹,
 G. Mornacchi³⁰, J.D. Morris⁷⁶, S.S. Mortensen³⁶, L. Morvaj¹⁴⁷, M. Mosidze^{51b}, J. Moss¹⁴²,
 K. Motohashi¹⁵⁶, R. Mount¹⁴², E. Mountricha²⁵, S.V. Mouraviev^{95,*}, E.J.W. Moyse⁸⁶, S. Muanza⁸⁵,
 R.D. Mudd¹⁸, F. Mueller¹⁰⁰, J. Mueller¹²⁴, R.S.P. Mueller⁹⁹, T. Mueller²⁸, D. Muenstermann⁷²,
 P. Mullen⁵³, G.A. Mullier¹⁷, F.J. Munoz Sanchez⁸⁴, J.A. Murillo Quijada¹⁸, W.J. Murray^{169,130},
 H. Musheghyan⁵⁴, A.G. Myagkov^{129,ac}, M. Myska¹²⁷, B.P. Nachman¹⁴², O. Nackenhorst⁴⁹, J. Nadal⁵⁴,
 K. Nagai¹¹⁹, R. Nagai^{66,w}, Y. Nagai⁸⁵, K. Nagano⁶⁶, Y. Nagasaka⁵⁹, K. Nagata¹⁵⁹, M. Nagel¹⁰⁰,
 E. Nagy⁸⁵, A.M. Nairz³⁰, Y. Nakahama³⁰, K. Nakamura⁶⁶, T. Nakamura¹⁵⁴, I. Nakano¹¹¹,
 H. Namasivayam⁴¹, R.F. Naranjo Garcia⁴², R. Narayan³¹, D.I. Narrias Villar^{58a}, I. Naryshkin¹²²,
 T. Naumann⁴², G. Navarro¹⁶¹, R. Nayyar⁷, H.A. Neal⁸⁹, P.Yu. Nechaeva⁹⁵, T.J. Neep⁸⁴, P.D. Nef¹⁴²,
 A. Negri^{120a,120b}, M. Negrini^{20a}, S. Nektarijevic¹⁰⁵, C. Nellist¹¹⁶, A. Nelson¹⁶², S. Nemecek¹²⁶,
 P. Nemethy¹⁰⁹, A.A. Nepomuceno^{24a}, M. Nessi^{30,ad}, M.S. Neubauer¹⁶⁴, M. Neumann¹⁷⁴, R.M. Neves¹⁰⁹,
 P. Nevski²⁵, P.R. Newman¹⁸, D.H. Nguyen⁶, R.B. Nickerson¹¹⁹, R. Nicolaidou¹³⁵, B. Nicquevert³⁰,
 J. Nielsen¹³⁶, A. Nikiforov¹⁶, V. Nikolaenko^{129,ac}, I. Nikolic-Audit⁸⁰, K. Nikolopoulos¹⁸, J.K. Nilsen¹¹⁸,
 P. Nilsson²⁵, Y. Ninomiya¹⁵⁴, A. Nisati^{131a}, R. Nisius¹⁰⁰, T. Nobe¹⁵⁴, L. Nodulman⁶, D. Nole^{91a,91b},
 M. Nomachi¹¹⁷, I. Nomidis²⁹, T. Nooney⁷⁶, S. Norberg¹¹², M. Nordberg³⁰, O. Novgorodova⁴⁴,
 S. Nowak¹⁰⁰, M. Nozaki⁶⁶, L. Nozka¹¹⁴, K. Ntekas¹⁰, E. Nurse⁷⁸, F. Nuti⁸⁸, F. O'grady⁷,
 D.C. O'Neil¹⁴¹, A.A. O'Rourke⁴², V. O'Shea⁵³, F.G. Oakham^{29,d}, H. Oberlack¹⁰⁰, T. Obermann²¹,
 J. Ocariz⁸⁰, A. Ochi⁶⁷, I. Ochoa³⁵, J.P. Ochoa-Ricoux^{32a}, S. Oda⁷⁰, S. Odaka⁶⁶, H. Ogren⁶¹, A. Oh⁸⁴,
 S.H. Oh⁴⁵, C.C. Ohm¹⁵, H. Ohman¹⁶⁵, H. Oide³⁰, H. Okawa¹⁵⁹, Y. Okumura³¹, T. Okuyama⁶⁶,
 A. Olariu^{26b}, L.F. Oleiro Seabra^{125a}, S.A. Olivares Pino⁴⁶, D. Oliveira Damazio²⁵, A. Olszewski³⁹,
 J. Olszowska³⁹, A. Onofre^{125a,125e}, K. Onogi¹⁰², P.U.E. Onyisi^{31,s}, C.J. Oram^{158a}, M.J. Oreglia³¹,
 Y. Oren¹⁵², D. Orestano^{133a,133b}, N. Orlando^{60b}, R.S. Orr¹⁵⁷, B. Osculati^{50a,50b}, R. Ospanov⁸⁴,
 G. Otero y Garzon²⁷, H. Otono⁷⁰, M. Ouchrif^{134d}, F. Ould-Saada¹¹⁸, A. Ouraou¹³⁵, K.P. Oussoren¹⁰⁶,
 Q. Ouyang^{33a}, A. Ovcharova¹⁵, M. Owen⁵³, R.E. Owen¹⁸, V.E. Ozcan^{19a}, N. Ozturk⁸, K. Pachal¹⁴¹,
 A. Pacheco Pages¹², C. Padilla Aranda¹², M. Pagáčová⁴⁸, S. Pagan Griso¹⁵, F. Paige²⁵, P. Pais⁸⁶,
 K. Pajchel¹¹⁸, G. Palacino^{158b}, S. Palestini³⁰, M. Palka^{38b}, D. Pallin³⁴, A. Palma^{125a,125b},
 E.St. Panagiotopoulou¹⁰, C.E. Pandini⁸⁰, J.G. Panduro Vazquez⁷⁷, P. Pani^{145a,145b}, S. Panitkin²⁵,
 D. Pantea^{26b}, L. Paolozzi⁴⁹, Th.D. Papadopoulou¹⁰, K. Papageorgiou¹⁵³, A. Paramonov⁶,
 D. Paredes Hernandez¹⁷⁵, M.A. Parker²⁸, K.A. Parker¹³⁸, F. Parodi^{50a,50b}, J.A. Parsons³⁵, U. Parzefall⁴⁸,
 V. Pascuzzi¹⁵⁷, E. Pasqualucci^{131a}, S. Passaggio^{50a}, F. Pastore^{133a,133b,*}, Fr. Pastore⁷⁷, G. Pásztor²⁹,
 S. Pataria¹⁷⁴, N.D. Patel¹⁴⁹, J.R. Pater⁸⁴, T. Pauly³⁰, J. Pearce¹⁶⁸, B. Pearson¹¹², L.E. Pedersen³⁶,
 M. Pedersen¹¹⁸, S. Pedraza Lopez¹⁶⁶, R. Pedro^{125a,125b}, S.V. Peleganchuk^{108,c}, D. Pelikan¹⁶⁵, O. Penc¹²⁶,
 C. Peng^{33a}, H. Peng^{33b}, J. Penwell⁶¹, B.S. Peralva^{24b}, D.V. Perepelitsa²⁵, E. Perez Codina^{158a},
 L. Perini^{91a,91b}, H. Pernegger³⁰, S. Perrella^{103a,103b}, R. Peschke⁴², V.D. Peshekhonov⁶⁵, K. Peters³⁰,
 R.F.Y. Peters⁸⁴, B.A. Petersen³⁰, T.C. Petersen³⁶, E. Petit⁵⁵, A. Petridis¹, C. Petridou¹⁵³, P. Petroff¹¹⁶,
 E. Petrolo^{131a}, F. Petrucci^{133a,133b}, N.E. Pettersson¹⁵⁶, A. Peyaud¹³⁵, R. Pezoa^{32b}, P.W. Phillips¹³⁰,
 G. Piacquadio¹⁴², E. Pianori¹⁶⁹, A. Picazio⁸⁶, E. Piccaro⁷⁶, M. Piccinini^{20a,20b}, M.A. Pickering¹¹⁹,
 R. Piegaia²⁷, J.E. Pilcher³¹, A.D. Pilkington⁸⁴, A.W.J. Pin⁸⁴, J. Pina^{125a,125b,125d},
 M. Pinamonti^{163a,163c,ae}, J.L. Pinfold³, A. Pingel³⁶, S. Pires⁸⁰, H. Pirumov⁴², M. Pitt¹⁷¹, L. Plazak^{143a},
 M.-A. Pleier²⁵, V. Pleskot⁸³, E. Plotnikova⁶⁵, P. Plucinski^{145a,145b}, D. Pluth⁶⁴, R. Poettgen^{145a,145b},
 L. Poggioli¹¹⁶, D. Pohl²¹, G. Polesello^{120a}, A. Poley⁴², A. Policicchio^{37a,37b}, R. Polifka¹⁵⁷, A. Polini^{20a},
 C.S. Pollard⁵³, V. Polychronakos²⁵, K. Pommès³⁰, L. Pontecorvo^{131a}, B.G. Pope⁹⁰, G.A. Popeneciu^{26c},
 D.S. Popovic¹³, A. Poppleton³⁰, S. Pospisil¹²⁷, K. Potamianos¹⁵, I.N. Potrap⁶⁵, C.J. Potter²⁸,
 C.T. Potter¹¹⁵, G. Poulard³⁰, J. Poveda³⁰, V. Pozdnyakov⁶⁵, M.E. Pozo Astigarraga³⁰, P. Pralavorio⁸⁵,
 A. Pranko¹⁵, S. Prell⁶⁴, D. Price⁸⁴, L.E. Price⁶, M. Primavera^{73a}, S. Prince⁸⁷, M. Proissl⁴⁶,
 K. Prokofiev^{60c}, F. Prokoshin^{32b}, S. Protopopescu²⁵, J. Proudfoot⁶, M. Przybycien^{38a}, D. Puudu^{133a,133b},

D. Puldon¹⁴⁷, M. Purohit^{25,af}, P. Puzo¹¹⁶, J. Qian⁸⁹, G. Qin⁵³, Y. Qin⁸⁴, A. Quadt⁵⁴, D.R. Quarrie¹⁵,
 W.B. Quayle^{163a,163b}, M. Queitsch-Maitland⁸⁴, D. Quilty⁵³, S. Raddum¹¹⁸, V. Radeka²⁵, V. Radescu⁴²,
 S.K. Radhakrishnan¹⁴⁷, P. Radloff¹¹⁵, P. Rados⁸⁸, F. Ragusa^{91a,91b}, G. Rahal¹⁷⁷, S. Rajagopalan²⁵,
 M. Rammensee³⁰, C. Rangel-Smith¹⁶⁵, M.G. Ratti^{91a,91b}, F. Rauscher⁹⁹, S. Rave⁸³, T. Ravenscroft⁵³,
 M. Raymond³⁰, A.L. Read¹¹⁸, N.P. Readioff⁷⁴, D.M. Rebuzzi^{120a,120b}, A. Redelbach¹⁷³, G. Redlinger²⁵,
 R. Reece¹³⁶, K. Reeves⁴¹, L. Rehnisch¹⁶, J. Reichert¹²¹, H. Reisin²⁷, C. Rembser³⁰, H. Ren^{33a},
 M. Rescigno^{131a}, S. Resconi^{91a}, O.L. Rezanova^{108,c}, P. Reznicek¹²⁸, R. Rezvani⁹⁴, R. Richter¹⁰⁰,
 S. Richter⁷⁸, E. Richter-Was^{38b}, O. Ricken²¹, M. Ridel⁸⁰, P. Rieck¹⁶, C.J. Riegel¹⁷⁴, J. Rieger⁵⁴,
 O. Rifki¹¹², M. Rijssenbeek¹⁴⁷, A. Rimoldi^{120a,120b}, L. Rinaldi^{20a}, B. Ristić⁴⁹, E. Ritsch³⁰, I. Riu¹²,
 F. Rizatdinova¹¹³, E. Rizvi⁷⁶, S.H. Robertson^{87,l}, A. Robichaud-Veronneau⁸⁷, D. Robinson²⁸,
 J.E.M. Robinson⁴², A. Robson⁵³, C. Roda^{123a,123b}, Y. Rodina⁸⁵, A. Rodriguez Perez¹²,
 D. Rodriguez Rodriguez¹⁶⁶, S. Roe³⁰, C.S. Rogan⁵⁷, O. Røhne¹¹⁸, A. Romaniouk⁹⁷, M. Romano^{20a,20b},
 S.M. Romano Saez³⁴, E. Romero Adam¹⁶⁶, N. Rompotis¹³⁷, M. Ronzani⁴⁸, L. Roos⁸⁰, E. Ros¹⁶⁶,
 S. Rosati^{131a}, K. Rosbach⁴⁸, P. Rose¹³⁶, O. Rosenthal¹⁴⁰, V. Rossetti^{145a,145b}, E. Rossi^{103a,103b},
 L.P. Rossi^{50a}, J.H.N. Rosten²⁸, R. Rosten¹³⁷, M. Rotaru^{26b}, I. Roth¹⁷¹, J. Rothberg¹³⁷, D. Rousseau¹¹⁶,
 C.R. Royon¹³⁵, A. Rozanov⁸⁵, Y. Rozen¹⁵¹, X. Ruan^{144c}, F. Rubbo¹⁴², I. Rubinskiy⁴², V.I. Rud⁹⁸,
 M.S. Rudolph¹⁵⁷, F. Rühr⁴⁸, A. Ruiz-Martinez³⁰, Z. Rurikova⁴⁸, N.A. Rusakovich⁶⁵, A. Ruschke⁹⁹,
 H.L. Russell¹³⁷, J.P. Rutherford⁷, N. Ruthmann³⁰, Y.F. Ryabov¹²², M. Rybar¹⁶⁴, G. Rybkin¹¹⁶,
 N.C. Ryder¹¹⁹, S. Ryu⁶, A. Ryzhov¹²⁹, A.F. Saavedra¹⁴⁹, G. Sabato¹⁰⁶, S. Sacerdoti²⁷,
 H.F.W. Sadrozinski¹³⁶, R. Sadykov⁶⁵, F. Safai Tehrani^{131a}, P. Saha¹⁰⁷, M. Sahinsoy^{58a}, M. Saimpert¹³⁵,
 T. Saito¹⁵⁴, H. Sakamoto¹⁵⁴, Y. Sakurai¹⁷⁰, G. Salamanna^{133a,133b}, A. Salamon^{132a},
 J.E. Salazar Loyola^{32b}, D. Salek¹⁰⁶, P.H. Sales De Bruin¹³⁷, D. Salihagic¹⁰⁰, A. Salmikov¹⁴², J. Salt¹⁶⁶,
 D. Salvatore^{37a,37b}, F. Salvatore¹⁴⁸, A. Salvucci^{60a}, A. Salzburger³⁰, D. Sammel⁴⁸, D. Sampsonidis¹⁵³,
 A. Sanchez^{103a,103b}, J. Sánchez¹⁶⁶, V. Sanchez Martinez¹⁶⁶, H. Sandaker¹¹⁸, R.L. Sandbach⁷⁶,
 H.G. Sander⁸³, M.P. Sanders⁹⁹, M. Sandhoff¹⁷⁴, C. Sandoval¹⁶¹, R. Sandstroem¹⁰⁰, D.P.C. Sankey¹³⁰,
 M. Sannino^{50a,50b}, A. Sansoni⁴⁷, C. Santoni³⁴, R. Santonico^{132a,132b}, H. Santos^{125a},
 I. Santoyo Castillo¹⁴⁸, K. Sapp¹²⁴, A. Saponov⁶⁵, J.G. Saraiva^{125a,125d}, B. Sarrazin²¹, O. Sasaki⁶⁶,
 Y. Sasaki¹⁵⁴, K. Sato¹⁵⁹, G. Sauvage^{5,*}, E. Sauvan⁵, G. Savage⁷⁷, P. Savard^{157,d}, C. Sawyer¹³⁰,
 L. Sawyer^{79,o}, J. Saxon³¹, C. Sbarra^{20a}, A. Sbrizzi^{20a,20b}, T. Scanlon⁷⁸, D.A. Scannicchio¹⁶²,
 M. Scarcella¹⁴⁹, V. Scarfone^{37a,37b}, J. Schaarschmidt¹⁷¹, P. Schacht¹⁰⁰, D. Schaefer³⁰, R. Schaefer⁴²,
 J. Schaeffer⁸³, S. Schaepe²¹, S. Schaezel^{58b}, U. Schäfer⁸³, A.C. Schaffer¹¹⁶, D. Schaile⁹⁹,
 R.D. Schamberger¹⁴⁷, V. Scharf^{58a}, V.A. Schegelsky¹²², D. Scheirich¹²⁸, M. Schernau¹⁶²,
 C. Schiavi^{50a,50b}, C. Schillo⁴⁸, M. Schioppa^{37a,37b}, S. Schlenker³⁰, K. Schmieden³⁰, C. Schmitt⁸³,
 S. Schmitt⁴², S. Schmitz⁸³, B. Schneider^{158a}, Y.J. Schnellbach⁷⁴, U. Schnoor⁴⁸, L. Schoeffel¹³⁵,
 A. Schoening^{58b}, B.D. Schoenrock⁹⁰, E. Schopf²¹, A.L.S. Schorlemmer⁴³, M. Schott⁸³, D. Schouten^{158a},
 J. Schovancova⁸, S. Schramm⁴⁹, M. Schreyer¹⁷³, N. Schuh⁸³, M.J. Schultens²¹,
 H.-C. Schultz-Coulon^{58a}, H. Schulz¹⁶, M. Schumacher⁴⁸, B.A. Schumm¹³⁶, Ph. Schune¹³⁵,
 C. Schwanenberger⁸⁴, A. Schwartzman¹⁴², T.A. Schwarz⁸⁹, Ph. Schwegler¹⁰⁰, H. Schweiger⁸⁴,
 Ph. Schwemling¹³⁵, R. Schwienhorst⁹⁰, J. Schwindling¹³⁵, T. Schwindt²¹, G. Sciolla²³, F. Scuri^{123a,123b},
 F. Scutti⁸⁸, J. Searcy⁸⁹, P. Seema²¹, S.C. Seidel¹⁰⁴, A. Seiden¹³⁶, F. Seifert¹²⁷, J.M. Seixas^{24a},
 G. Sekhniaidze^{103a}, K. Sekhon⁸⁹, S.J. Sekula⁴⁰, D.M. Seliverstov^{122,*}, N. Semprini-Cesari^{20a,20b},
 C. Serfon³⁰, L. Serin¹¹⁶, L. Serkin^{163a,163b}, M. Sessa^{133a,133b}, R. Seuster^{158a}, H. Severini¹¹², T. Sfiligoj⁷⁵,
 F. Sforza³⁰, A. Sfyrla⁴⁹, E. Shabalina⁵⁴, N.W. Shaikh^{145a,145b}, L.Y. Shan^{33a}, R. Shang¹⁶⁴, J.T. Shank²²,
 M. Shapiro¹⁵, P.B. Shatalov⁹⁶, K. Shaw^{163a,163b}, S.M. Shaw⁸⁴, A. Shcherbakova^{145a,145b}, C.Y. Shehu¹⁴⁸,
 P. Sherwood⁷⁸, L. Shi^{150,ag}, S. Shimizu⁶⁷, C.O. Shimmin¹⁶², M. Shimojima¹⁰¹, M. Shiyakova^{65,ah},
 A. Shmeleva⁹⁵, D. Shoaleh Saadi⁹⁴, M.J. Shochet³¹, S. Shojai^{91a,91b}, S. Shrestha¹¹⁰, E. Shulga⁹⁷,
 M.A. Shupe⁷, P. Sicho¹²⁶, P.E. Sidebo¹⁴⁶, O. Sidiropoulou¹⁷³, D. Sidorov¹¹³, A. Sidoti^{20a,20b},

F. Siegert⁴⁴, Dj. Sijacki¹³, J. Silva^{125a,125d}, S.B. Silverstein^{145a}, V. Simak¹²⁷, O. Simard⁵, Lj. Simic¹³, S. Simion¹¹⁶, E. Simioni⁸³, B. Simmons⁷⁸, D. Simon³⁴, M. Simon⁸³, P. Sinervo¹⁵⁷, N.B. Sinev¹¹⁵, M. Sioli^{20a,20b}, G. Siragusa¹⁷³, S.Yu. Sivoklov⁹⁸, J. Sjölin^{145a,145b}, T.B. Sjursen¹⁴, M.B. Skinner⁷², H.P. Skottowe⁵⁷, P. Skubic¹¹², M. Slater¹⁸, T. Slavicek¹²⁷, M. Slawinska¹⁰⁶, K. Sliwa¹⁶⁰, V. Smakhtin¹⁷¹, B.H. Smart⁵, L. Smestad¹⁴, S.Yu. Smirnov⁹⁷, Y. Smirnov⁹⁷, L.N. Smirnova^{98.ai}, O. Smirnova⁸¹, M.N.K. Smith³⁵, R.W. Smith³⁵, M. Smizanska⁷², K. Smolek¹²⁷, A.A. Snesarev⁹⁵, G. Snidero⁷⁶, S. Snyder²⁵, R. Sobie^{168.l}, F. Socher⁴⁴, A. Soffer¹⁵², D.A. Soh^{150.ag}, G. Sokhrannyi⁷⁵, C.A. Solans Sanchez³⁰, M. Solar¹²⁷, E. Yu. Soldatov⁹⁷, U. Soldevila¹⁶⁶, A.A. Solodkov¹²⁹, A. Soloshenko⁶⁵, O.V. Solovyanov¹²⁹, V. Solovyev¹²², P. Sommer⁴⁸, H.Y. Song^{33b,z}, N. Soni¹, A. Sood¹⁵, A. Sopczak¹²⁷, V. Sopko¹²⁷, V. Sorin¹², D. Sosa^{58b}, C.L. Sotiropoulou^{123a,123b}, R. Soualah^{163a,163c}, A.M. Soukharev^{108.c}, D. South⁴², B.C. Sowden⁷⁷, S. Spagnolo^{73a,73b}, M. Spalla^{123a,123b}, M. Spangenberg¹⁶⁹, F. Spanò⁷⁷, D. Sperlich¹⁶, F. Spettel¹⁰⁰, R. Spighi^{20a}, G. Spigo³⁰, L.A. Spiller⁸⁸, M. Spousta¹²⁸, R.D. St. Denis^{53,*}, A. Stabile^{91a}, S. Staerz³⁰, J. Stahlman¹²¹, R. Stamen^{58a}, S. Stamm¹⁶, E. Stanecka³⁹, R.W. Stanek⁶, C. Stanescu^{133a}, M. Stanescu-Bellu⁴², M.M. Stanitzki⁴², S. Stapnes¹¹⁸, E.A. Starchenko¹²⁹, G.H. Stark³¹, J. Stark⁵⁵, P. Staroba¹²⁶, P. Starovoitov^{58a}, R. Staszewski³⁹, P. Steinberg²⁵, B. Stelzer¹⁴¹, H.J. Stelzer³⁰, O. Stelzer-Chilton^{158a}, H. Stenzel⁵², G.A. Stewart⁵³, J.A. Stillings²¹, M.C. Stockton⁸⁷, M. Stoebe⁸⁷, G. Stoica^{26b}, P. Stolte⁵⁴, S. Stonjek¹⁰⁰, A.R. Stradling⁸, A. Straessner⁴⁴, M.E. Stramaglia¹⁷, J. Strandberg¹⁴⁶, S. Strandberg^{145a,145b}, A. Strandlie¹¹⁸, M. Strauss¹¹², P. Strizenec^{143b}, R. Ströhmer¹⁷³, D.M. Strom¹¹⁵, R. Stroynowski⁴⁰, A. Strubig¹⁰⁵, S.A. Stucci¹⁷, B. Stugu¹⁴, N.A. Styles⁴², D. Su¹⁴², J. Su¹²⁴, R. Subramaniam⁷⁹, S. Suchek^{58a}, Y. Sugaya¹¹⁷, M. Suk¹²⁷, V.V. Sulin⁹⁵, S. Sultansoy^{4c}, T. Sumida⁶⁸, S. Sun⁵⁷, X. Sun^{33a}, J.E. Sundermann⁴⁸, K. Suruliz¹⁴⁸, G. Susinno^{37a,37b}, M.R. Sutton¹⁴⁸, S. Suzuki⁶⁶, M. Svatos¹²⁶, M. Swiatlowski³¹, I. Sykora^{143a}, T. Sykora¹²⁸, D. Ta⁴⁸, C. Taccini^{133a,133b}, K. Tackmann⁴², J. Taenzer¹⁵⁷, A. Taffard¹⁶², R. Tafirout^{158a}, N. Taiblum¹⁵², H. Takai²⁵, R. Takashima⁶⁹, H. Takeda⁶⁷, T. Takeshita¹³⁹, Y. Takubo⁶⁶, M. Talby⁸⁵, A.A. Talyshv^{108.c}, J.Y.C. Tam¹⁷³, K.G. Tan⁸⁸, J. Tanaka¹⁵⁴, R. Tanaka¹¹⁶, S. Tanaka⁶⁶, B.B. Tannenwald¹¹⁰, S. Tapia Araya^{32b}, S. Tapprogge⁸³, S. Tarem¹⁵¹, G.F. Tartarelli^{91a}, P. Tas¹²⁸, M. Tasevsky¹²⁶, T. Tashiro⁶⁸, E. Tassi^{37a,37b}, A. Tavares Delgado^{125a,125b}, Y. Tayalati^{134d}, A.C. Taylor¹⁰⁴, G.N. Taylor⁸⁸, P.T.E. Taylor⁸⁸, W. Taylor^{158b}, F.A. Teischinger³⁰, P. Teixeira-Dias⁷⁷, K.K. Temming⁴⁸, D. Temple¹⁴¹, H. Ten Kate³⁰, P.K. Teng¹⁵⁰, J.J. Teoh¹¹⁷, F. Tepel¹⁷⁴, S. Terada⁶⁶, K. Terashi¹⁵⁴, J. Terron⁸², S. Terzo¹⁰⁰, M. Testa⁴⁷, R.J. Teuscher^{157.l}, T. Theveneaux-Pelzer⁸⁵, J.P. Thomas¹⁸, J. Thomas-Wilsker⁷⁷, E.N. Thompson³⁵, P.D. Thompson¹⁸, R.J. Thompson⁸⁴, A.S. Thompson⁵³, L.A. Thomsen¹⁷⁵, E. Thomson¹²¹, M. Thomson²⁸, M.J. Tibbetts¹⁵, R.E. Ticse Torres⁸⁵, V.O. Tikhomirov^{95.aj}, Yu.A. Tikhonov^{108.c}, S. Timoshenko⁹⁷, E. Tiouchichine⁸⁵, P. Tipton¹⁷⁵, S. Tisserant⁸⁵, K. Todome¹⁵⁶, T. Todorov^{5,*}, S. Todorova-Nova¹²⁸, J. Tojo⁷⁰, S. Tokár^{143a}, K. Tokushuku⁶⁶, E. Tolley⁵⁷, L. Tomlinson⁸⁴, M. Tomoto¹⁰², L. Tompkins^{142.ak}, K. Toms¹⁰⁴, B. Tong⁵⁷, E. Torrence¹¹⁵, H. Torres¹⁴¹, E. Torró Pastor¹³⁷, J. Toth^{85.al}, F. Touchard⁸⁵, D.R. Tovey¹³⁸, T. Trefzger¹⁷³, L. Tremblet³⁰, A. Tricoli³⁰, I.M. Trigger^{158a}, S. Trincaz-Duvoid⁸⁰, M.F. Tripiana¹², W. Trischuk¹⁵⁷, B. Trocme⁵⁵, A. Trofymov⁴², C. Troncon^{91a}, M. Trottier-McDonald¹⁵, M. Trovatelli¹⁶⁸, L. Truong^{163a,163b}, M. Trzebinski³⁹, A. Trzupek³⁹, J.C-L. Tseng¹¹⁹, P.V. Tsiarehka⁹², G. Tsipolitis¹⁰, N. Tsirintanis⁹, S. Tsiskaridze¹², V. Tsiskaridze⁴⁸, E.G. Tskhadadze^{51a}, K.M. Tsui^{60a}, I.I. Tsukerman⁹⁶, V. Tsulaia¹⁵, S. Tsuno⁶⁶, D. Tsybychev¹⁴⁷, A. Tudorache^{26b}, V. Tudorache^{26b}, A.N. Tuna⁵⁷, S.A. Tupputi^{20a,20b}, S. Turchikhin^{98.ai}, D. Turecek¹²⁷, D. Turgeman¹⁷¹, R. Turra^{91a,91b}, A.J. Turvey⁴⁰, P.M. Tuts³⁵, M. Tylmad^{145a,145b}, M. Tyndel¹³⁰, I. Ueda¹⁵⁴, R. Ueno²⁹, M. Ughetto^{145a,145b}, F. Ukegawa¹⁵⁹, G. Unal³⁰, A. Undrus²⁵, G. Unel¹⁶², F.C. Ungaro⁸⁸, Y. Unno⁶⁶, C. Unverdorben⁹⁹, J. Urban^{143b}, P. Urquijo⁸⁸, P. Urrejola⁸³, G. Usai⁸, A. Usanova⁶², L. Vacavant⁸⁵, V. Vacek¹²⁷, B. Vachon⁸⁷, C. Valderanis⁸³, E. Valdes Santurio^{145a,145b}, N. Valencic¹⁰⁶, S. Valentini^{20a,20b}, A. Valero¹⁶⁶, L. Valery¹², S. Valkar¹²⁸, S. Vallecorsa⁴⁹, J.A. Valls Ferrer¹⁶⁶, W. Van Den Wollenberg¹⁰⁶,

P.C. Van Der Deijl¹⁰⁶, R. van der Geer¹⁰⁶, H. van der Graaf¹⁰⁶, N. van Eldik¹⁵¹, P. van Gemmeren⁶, J. Van Nieuwkoop¹⁴¹, I. van Vulpen¹⁰⁶, M.C. van Woerden³⁰, M. Vanadia^{131a,131b}, W. Vandelli³⁰, R. Vanguri¹²¹, A. Vaniachine⁶, P. Vankov¹⁰⁶, G. Vardanyan¹⁷⁶, R. Vari^{131a}, E.W. Varnes⁷, T. Varol⁴⁰, D. Varouchas⁸⁰, A. Vartapetian⁸, K.E. Varvell¹⁴⁹, F. Vazeille³⁴, T. Vazquez Schroeder⁸⁷, J. Veatch⁷, L.M. Veloce¹⁵⁷, F. Veloso^{125a,125c}, S. Veneziano^{131a}, A. Ventura^{73a,73b}, M. Venturi¹⁶⁸, N. Venturi¹⁵⁷, A. Venturini²³, V. Vercesi^{120a}, M. Verducci^{131a,131b}, W. Verkerke¹⁰⁶, J.C. Vermeulen¹⁰⁶, A. Vest^{44.am}, M.C. Vetterli^{141.d}, O. Viazlo⁸¹, I. Vichou¹⁶⁴, T. Vickey¹³⁸, O.E. Vickey Boeriu¹³⁸, G.H.A. Viehhauser¹¹⁹, S. Viel¹⁵, R. Vigne⁶², M. Villa^{20a,20b}, M. Villaplana Perez^{91a,91b}, E. Vilucchi⁴⁷, M.G. Vincter²⁹, V.B. Vinogradov⁶⁵, I. Vivarelli¹⁴⁸, S. Vlachos¹⁰, M. Vlasak¹²⁷, M. Vogel¹⁷⁴, P. Vokac¹²⁷, G. Volpi^{123a,123b}, M. Volpi⁸⁸, H. von der Schmitt¹⁰⁰, E. von Toerne²¹, V. Vorobel¹²⁸, K. Vorobev⁹⁷, M. Vos¹⁶⁶, R. Voss³⁰, J.H. Vossebeld⁷⁴, N. Vranjes¹³, M. Vranjes Milosavljevic¹³, V. Vrba¹²⁶, M. Vreeswijk¹⁰⁶, R. Vuillermet³⁰, I. Vukotic³¹, Z. Vykydal¹²⁷, P. Wagner²¹, W. Wagner¹⁷⁴, H. Wahlberg⁷¹, S. Wahrmund⁴⁴, J. Wakabayashi¹⁰², J. Walder⁷², R. Walker⁹⁹, W. Walkowiak¹⁴⁰, V. Wallangen^{145a,145b}, C. Wang¹⁵⁰, C. Wang^{33d,85}, F. Wang¹⁷², H. Wang¹⁵, H. Wang⁴⁰, J. Wang⁴², J. Wang¹⁴⁹, K. Wang⁸⁷, R. Wang⁶, S.M. Wang¹⁵⁰, T. Wang²¹, T. Wang³⁵, X. Wang¹⁷⁵, C. Wanotayaroj¹¹⁵, A. Warburton⁸⁷, C.P. Ward²⁸, D.R. Wardrope⁷⁸, A. Washbrook⁴⁶, P.M. Watkins¹⁸, A.T. Watson¹⁸, I.J. Watson¹⁴⁹, M.F. Watson¹⁸, G. Watts¹³⁷, S. Watts⁸⁴, B.M. Waugh⁷⁸, S. Webb⁸³, M.S. Weber¹⁷, S.W. Weber¹⁷³, J.S. Webster⁶, A.R. Weidberg¹¹⁹, B. Weinert⁶¹, J. Weingarten⁵⁴, C. Weiser⁴⁸, H. Weits¹⁰⁶, P.S. Wells³⁰, T. Wenaus²⁵, T. Wengler³⁰, S. Wenig³⁰, N. Vermes²¹, M. Werner⁴⁸, P. Werner³⁰, M. Wessels^{58a}, J. Wetter¹⁶⁰, K. Whalen¹¹⁵, A.M. Wharton⁷², A. White⁸, M.J. White¹, R. White^{32b}, S. White^{123a,123b}, D. Whiteson¹⁶², F.J. Wickens¹³⁰, W. Wiedenmann¹⁷², M. Wielers¹³⁰, P. Wienemann²¹, C. Wiglesworth³⁶, L.A.M. Wiik-Fuchs²¹, A. Wildauer¹⁰⁰, H.G. Wilkens³⁰, H.H. Williams¹²¹, S. Williams¹⁰⁶, C. Willis⁹⁰, S. Willocq⁸⁶, J.A. Wilson¹⁸, I. Wingerter-Seez⁵, F. Winklmeier¹¹⁵, B.T. Winter²¹, M. Wittgen¹⁴², J. Wittkowski⁹⁹, S.J. Wollstadt⁸³, M.W. Wolter³⁹, H. Wolters^{125a,125c}, B.K. Wosiek³⁹, J. Wotschack³⁰, M.J. Woudstra⁸⁴, K.W. Wozniak³⁹, M. Wu⁵⁵, M. Wu³¹, S.L. Wu¹⁷², X. Wu⁴⁹, Y. Wu⁸⁹, T.R. Wyatt⁸⁴, B.M. Wynne⁴⁶, S. Xella³⁶, D. Xu^{33a}, L. Xu²⁵, B. Yabsley¹⁴⁹, S. Yacoob^{144a}, R. Yakabe⁶⁷, D. Yamaguchi¹⁵⁶, Y. Yamaguchi¹¹⁷, A. Yamamoto⁶⁶, S. Yamamoto¹⁵⁴, T. Yamanaka¹⁵⁴, K. Yamauchi¹⁰², Y. Yamazaki⁶⁷, Z. Yan²², H. Yang^{33e}, H. Yang¹⁷², Y. Yang¹⁵⁰, Z. Yang¹⁴, W-M. Yao¹⁵, Y.C. Yap⁸⁰, Y. Yasu⁶⁶, E. Yatsenko⁵, K.H. Yau Wong²¹, J. Ye⁴⁰, S. Ye²⁵, I. Yeletsikh⁶⁵, A.L. Yen⁵⁷, E. Yildirim⁴², K. Yorita¹⁷⁰, R. Yoshida⁶, K. Yoshihara¹²¹, C. Young¹⁴², C.J.S. Young³⁰, S. Youssef²², D.R. Yu¹⁵, J. Yu⁸, J.M. Yu⁸⁹, J. Yu⁶⁴, L. Yuan⁶⁷, S.P.Y. Yuen²¹, I. Yusuff^{28.an}, B. Zabinski³⁹, R. Zaidan^{33d}, A.M. Zaitsev^{129.ac}, N. Zakharchuk⁴², J. Zalieckas¹⁴, A. Zaman¹⁴⁷, S. Zambito⁵⁷, L. Zanello^{131a,131b}, D. Zanzi⁸⁸, C. Zeitnitz¹⁷⁴, M. Zeman¹²⁷, A. Zemla^{38a}, J.C. Zeng¹⁶⁴, Q. Zeng¹⁴², K. Zengel²³, O. Zenin¹²⁹, T. Ženiš^{143a}, D. Zerwas¹¹⁶, D. Zhang⁸⁹, F. Zhang¹⁷², G. Zhang^{33b,z}, H. Zhang^{33c}, J. Zhang⁶, L. Zhang⁴⁸, R. Zhang²¹, R. Zhang^{33b,ao}, X. Zhang^{33d}, Z. Zhang¹¹⁶, X. Zhao⁴⁰, Y. Zhao^{33d,116}, Z. Zhao^{33b}, A. Zhemchugov⁶⁵, J. Zhong¹¹⁹, B. Zhou⁸⁹, C. Zhou⁴⁵, L. Zhou³⁵, L. Zhou⁴⁰, M. Zhou¹⁴⁷, N. Zhou^{33f}, C.G. Zhu^{33d}, H. Zhu^{33a}, J. Zhu⁸⁹, Y. Zhu^{33b}, X. Zhuang^{33a}, K. Zhukov⁹⁵, A. Zibell¹⁷³, D. Zieminska⁶¹, N.I. Zimine⁶⁵, C. Zimmermann⁸³, S. Zimmermann⁴⁸, Z. Zinonos⁵⁴, M. Zinser⁸³, M. Ziolkowski¹⁴⁰, L. Živković¹³, G. Zobernig¹⁷², A. Zoccoli^{20a,20b}, M. zur Nedden¹⁶, G. Zurzolo^{103a,103b}, L. Zwalinski³⁰.

¹ Department of Physics, University of Adelaide, Adelaide, Australia

² Physics Department, SUNY Albany, Albany NY, United States of America

³ Department of Physics, University of Alberta, Edmonton AB, Canada

⁴ (a) Department of Physics, Ankara University, Ankara; (b) Istanbul Aydin University, Istanbul; (c)

Division of Physics, TOBB University of Economics and Technology, Ankara, Turkey

⁵ LAPP, CNRS/IN2P3 and Université Savoie Mont Blanc, Annecy-le-Vieux, France

- ⁶ High Energy Physics Division, Argonne National Laboratory, Argonne IL, United States of America
- ⁷ Department of Physics, University of Arizona, Tucson AZ, United States of America
- ⁸ Department of Physics, The University of Texas at Arlington, Arlington TX, United States of America
- ⁹ Physics Department, University of Athens, Athens, Greece
- ¹⁰ Physics Department, National Technical University of Athens, Zografou, Greece
- ¹¹ Institute of Physics, Azerbaijan Academy of Sciences, Baku, Azerbaijan
- ¹² Institut de Física d'Altes Energies (IFAE), The Barcelona Institute of Science and Technology, Barcelona, Spain, Spain
- ¹³ Institute of Physics, University of Belgrade, Belgrade, Serbia
- ¹⁴ Department for Physics and Technology, University of Bergen, Bergen, Norway
- ¹⁵ Physics Division, Lawrence Berkeley National Laboratory and University of California, Berkeley CA, United States of America
- ¹⁶ Department of Physics, Humboldt University, Berlin, Germany
- ¹⁷ Albert Einstein Center for Fundamental Physics and Laboratory for High Energy Physics, University of Bern, Bern, Switzerland
- ¹⁸ School of Physics and Astronomy, University of Birmingham, Birmingham, United Kingdom
- ¹⁹ ^(a) Department of Physics, Bogazici University, Istanbul; ^(b) Department of Physics Engineering, Gaziantep University, Gaziantep; ^(d) Istanbul Bilgi University, Faculty of Engineering and Natural Sciences, Istanbul, Turkey; ^(e) Bahcesehir University, Faculty of Engineering and Natural Sciences, Istanbul, Turkey, Turkey
- ²⁰ ^(a) INFN Sezione di Bologna; ^(b) Dipartimento di Fisica e Astronomia, Università di Bologna, Bologna, Italy
- ²¹ Physikalisches Institut, University of Bonn, Bonn, Germany
- ²² Department of Physics, Boston University, Boston MA, United States of America
- ²³ Department of Physics, Brandeis University, Waltham MA, United States of America
- ²⁴ ^(a) Universidade Federal do Rio De Janeiro COPPE/EE/IF, Rio de Janeiro; ^(b) Electrical Circuits Department, Federal University of Juiz de Fora (UFJF), Juiz de Fora; ^(c) Federal University of Sao Joao del Rei (UFSJ), Sao Joao del Rei; ^(d) Instituto de Fisica, Universidade de Sao Paulo, Sao Paulo, Brazil
- ²⁵ Physics Department, Brookhaven National Laboratory, Upton NY, United States of America
- ²⁶ ^(a) Transilvania University of Brasov, Brasov, Romania; ^(b) National Institute of Physics and Nuclear Engineering, Bucharest; ^(c) National Institute for Research and Development of Isotopic and Molecular Technologies, Physics Department, Cluj Napoca; ^(d) University Politehnica Bucharest, Bucharest; ^(e) West University in Timisoara, Timisoara, Romania
- ²⁷ Departamento de Física, Universidad de Buenos Aires, Buenos Aires, Argentina
- ²⁸ Cavendish Laboratory, University of Cambridge, Cambridge, United Kingdom
- ²⁹ Department of Physics, Carleton University, Ottawa ON, Canada
- ³⁰ CERN, Geneva, Switzerland
- ³¹ Enrico Fermi Institute, University of Chicago, Chicago IL, United States of America
- ³² ^(a) Departamento de Física, Pontificia Universidad Católica de Chile, Santiago; ^(b) Departamento de Física, Universidad Técnica Federico Santa María, Valparaíso, Chile
- ³³ ^(a) Institute of High Energy Physics, Chinese Academy of Sciences, Beijing; ^(b) Department of Modern Physics, University of Science and Technology of China, Anhui; ^(c) Department of Physics, Nanjing University, Jiangsu; ^(d) School of Physics, Shandong University, Shandong; ^(e) Department of Physics and Astronomy, Shanghai Key Laboratory for Particle Physics and Cosmology, Shanghai Jiao Tong University, Shanghai; (also affiliated with PKU-CHEP); ^(f) Physics Department, Tsinghua University, Beijing 100084, China
- ³⁴ Laboratoire de Physique Corpusculaire, Clermont Université and Université Blaise Pascal and

CNRS/IN2P3, Clermont-Ferrand, France

³⁵ Nevis Laboratory, Columbia University, Irvington NY, United States of America

³⁶ Niels Bohr Institute, University of Copenhagen, Kobenhavn, Denmark

³⁷ ^(a) INFN Gruppo Collegato di Cosenza, Laboratori Nazionali di Frascati; ^(b) Dipartimento di Fisica, Università della Calabria, Rende, Italy

³⁸ ^(a) AGH University of Science and Technology, Faculty of Physics and Applied Computer Science, Krakow; ^(b) Marian Smoluchowski Institute of Physics, Jagiellonian University, Krakow, Poland

³⁹ Institute of Nuclear Physics Polish Academy of Sciences, Krakow, Poland

⁴⁰ Physics Department, Southern Methodist University, Dallas TX, United States of America

⁴¹ Physics Department, University of Texas at Dallas, Richardson TX, United States of America

⁴² DESY, Hamburg and Zeuthen, Germany

⁴³ Institut für Experimentelle Physik IV, Technische Universität Dortmund, Dortmund, Germany

⁴⁴ Institut für Kern- und Teilchenphysik, Technische Universität Dresden, Dresden, Germany

⁴⁵ Department of Physics, Duke University, Durham NC, United States of America

⁴⁶ SUPA - School of Physics and Astronomy, University of Edinburgh, Edinburgh, United Kingdom

⁴⁷ INFN Laboratori Nazionali di Frascati, Frascati, Italy

⁴⁸ Fakultät für Mathematik und Physik, Albert-Ludwigs-Universität, Freiburg, Germany

⁴⁹ Section de Physique, Université de Genève, Geneva, Switzerland

⁵⁰ ^(a) INFN Sezione di Genova; ^(b) Dipartimento di Fisica, Università di Genova, Genova, Italy

⁵¹ ^(a) E. Andronikashvili Institute of Physics, Iv. Javakhishvili Tbilisi State University, Tbilisi; ^(b) High Energy Physics Institute, Tbilisi State University, Tbilisi, Georgia

⁵² II Physikalisches Institut, Justus-Liebig-Universität Giessen, Giessen, Germany

⁵³ SUPA - School of Physics and Astronomy, University of Glasgow, Glasgow, United Kingdom

⁵⁴ II Physikalisches Institut, Georg-August-Universität, Göttingen, Germany

⁵⁵ Laboratoire de Physique Subatomique et de Cosmologie, Université Grenoble-Alpes, CNRS/IN2P3, Grenoble, France

⁵⁶ Department of Physics, Hampton University, Hampton VA, United States of America

⁵⁷ Laboratory for Particle Physics and Cosmology, Harvard University, Cambridge MA, United States of America

⁵⁸ ^(a) Kirchhoff-Institut für Physik, Ruprecht-Karls-Universität Heidelberg, Heidelberg; ^(b)

Physikalisches Institut, Ruprecht-Karls-Universität Heidelberg, Heidelberg; ^(c) ZITI Institut für technische Informatik, Ruprecht-Karls-Universität Heidelberg, Mannheim, Germany

⁵⁹ Faculty of Applied Information Science, Hiroshima Institute of Technology, Hiroshima, Japan

⁶⁰ ^(a) Department of Physics, The Chinese University of Hong Kong, Shatin, N.T., Hong Kong; ^(b)

Department of Physics, The University of Hong Kong, Hong Kong; ^(c) Department of Physics, The Hong Kong University of Science and Technology, Clear Water Bay, Kowloon, Hong Kong, China

⁶¹ Department of Physics, Indiana University, Bloomington IN, United States of America

⁶² Institut für Astro- und Teilchenphysik, Leopold-Franzens-Universität, Innsbruck, Austria

⁶³ University of Iowa, Iowa City IA, United States of America

⁶⁴ Department of Physics and Astronomy, Iowa State University, Ames IA, United States of America

⁶⁵ Joint Institute for Nuclear Research, JINR Dubna, Dubna, Russia

⁶⁶ KEK, High Energy Accelerator Research Organization, Tsukuba, Japan

⁶⁷ Graduate School of Science, Kobe University, Kobe, Japan

⁶⁸ Faculty of Science, Kyoto University, Kyoto, Japan

⁶⁹ Kyoto University of Education, Kyoto, Japan

⁷⁰ Department of Physics, Kyushu University, Fukuoka, Japan

⁷¹ Instituto de Física La Plata, Universidad Nacional de La Plata and CONICET, La Plata, Argentina

- 72 Physics Department, Lancaster University, Lancaster, United Kingdom
- 73 ^(a) INFN Sezione di Lecce; ^(b) Dipartimento di Matematica e Fisica, Università del Salento, Lecce, Italy
- 74 Oliver Lodge Laboratory, University of Liverpool, Liverpool, United Kingdom
- 75 Department of Physics, Jožef Stefan Institute and University of Ljubljana, Ljubljana, Slovenia
- 76 School of Physics and Astronomy, Queen Mary University of London, London, United Kingdom
- 77 Department of Physics, Royal Holloway University of London, Surrey, United Kingdom
- 78 Department of Physics and Astronomy, University College London, London, United Kingdom
- 79 Louisiana Tech University, Ruston LA, United States of America
- 80 Laboratoire de Physique Nucléaire et de Hautes Energies, UPMC and Université Paris-Diderot and CNRS/IN2P3, Paris, France
- 81 Fysiska institutionen, Lunds universitet, Lund, Sweden
- 82 Departamento de Física Teórica C-15, Universidad Autónoma de Madrid, Madrid, Spain
- 83 Institut für Physik, Universität Mainz, Mainz, Germany
- 84 School of Physics and Astronomy, University of Manchester, Manchester, United Kingdom
- 85 CPPM, Aix-Marseille Université and CNRS/IN2P3, Marseille, France
- 86 Department of Physics, University of Massachusetts, Amherst MA, United States of America
- 87 Department of Physics, McGill University, Montreal QC, Canada
- 88 School of Physics, University of Melbourne, Victoria, Australia
- 89 Department of Physics, The University of Michigan, Ann Arbor MI, United States of America
- 90 Department of Physics and Astronomy, Michigan State University, East Lansing MI, United States of America
- 91 ^(a) INFN Sezione di Milano; ^(b) Dipartimento di Fisica, Università di Milano, Milano, Italy
- 92 B.I. Stepanov Institute of Physics, National Academy of Sciences of Belarus, Minsk, Republic of Belarus
- 93 National Scientific and Educational Centre for Particle and High Energy Physics, Minsk, Republic of Belarus
- 94 Group of Particle Physics, University of Montreal, Montreal QC, Canada
- 95 P.N. Lebedev Physical Institute of the Russian Academy of Sciences, Moscow, Russia
- 96 Institute for Theoretical and Experimental Physics (ITEP), Moscow, Russia
- 97 National Research Nuclear University MEPhI, Moscow, Russia
- 98 D.V. Skobeltsyn Institute of Nuclear Physics, M.V. Lomonosov Moscow State University, Moscow, Russia
- 99 Fakultät für Physik, Ludwig-Maximilians-Universität München, München, Germany
- 100 Max-Planck-Institut für Physik (Werner-Heisenberg-Institut), München, Germany
- 101 Nagasaki Institute of Applied Science, Nagasaki, Japan
- 102 Graduate School of Science and Kobayashi-Maskawa Institute, Nagoya University, Nagoya, Japan
- 103 ^(a) INFN Sezione di Napoli; ^(b) Dipartimento di Fisica, Università di Napoli, Napoli, Italy
- 104 Department of Physics and Astronomy, University of New Mexico, Albuquerque NM, United States of America
- 105 Institute for Mathematics, Astrophysics and Particle Physics, Radboud University Nijmegen/Nikhef, Nijmegen, Netherlands
- 106 Nikhef National Institute for Subatomic Physics and University of Amsterdam, Amsterdam, Netherlands
- 107 Department of Physics, Northern Illinois University, DeKalb IL, United States of America
- 108 Budker Institute of Nuclear Physics, SB RAS, Novosibirsk, Russia
- 109 Department of Physics, New York University, New York NY, United States of America

- ¹¹⁰ Ohio State University, Columbus OH, United States of America
- ¹¹¹ Faculty of Science, Okayama University, Okayama, Japan
- ¹¹² Homer L. Dodge Department of Physics and Astronomy, University of Oklahoma, Norman OK, United States of America
- ¹¹³ Department of Physics, Oklahoma State University, Stillwater OK, United States of America
- ¹¹⁴ Palacký University, RCPTM, Olomouc, Czech Republic
- ¹¹⁵ Center for High Energy Physics, University of Oregon, Eugene OR, United States of America
- ¹¹⁶ LAL, Univ. Paris-Sud, CNRS/IN2P3, Université Paris-Saclay, Orsay, France
- ¹¹⁷ Graduate School of Science, Osaka University, Osaka, Japan
- ¹¹⁸ Department of Physics, University of Oslo, Oslo, Norway
- ¹¹⁹ Department of Physics, Oxford University, Oxford, United Kingdom
- ¹²⁰ ^(a) INFN Sezione di Pavia; ^(b) Dipartimento di Fisica, Università di Pavia, Pavia, Italy
- ¹²¹ Department of Physics, University of Pennsylvania, Philadelphia PA, United States of America
- ¹²² National Research Centre "Kurchatov Institute" B.P.Konstantinov Petersburg Nuclear Physics Institute, St. Petersburg, Russia
- ¹²³ ^(a) INFN Sezione di Pisa; ^(b) Dipartimento di Fisica E. Fermi, Università di Pisa, Pisa, Italy
- ¹²⁴ Department of Physics and Astronomy, University of Pittsburgh, Pittsburgh PA, United States of America
- ¹²⁵ ^(a) Laboratório de Instrumentação e Física Experimental de Partículas - LIP, Lisboa; ^(b) Faculdade de Ciências, Universidade de Lisboa, Lisboa; ^(c) Department of Physics, University of Coimbra, Coimbra; ^(d) Centro de Física Nuclear da Universidade de Lisboa, Lisboa; ^(e) Departamento de Física, Universidade do Minho, Braga; ^(f) Departamento de Física Teórica y del Cosmos and CAFPE, Universidad de Granada, Granada (Spain); ^(g) Dep Física and CEFITEC of Faculdade de Ciências e Tecnologia, Universidade Nova de Lisboa, Caparica, Portugal
- ¹²⁶ Institute of Physics, Academy of Sciences of the Czech Republic, Praha, Czech Republic
- ¹²⁷ Czech Technical University in Prague, Praha, Czech Republic
- ¹²⁸ Faculty of Mathematics and Physics, Charles University in Prague, Praha, Czech Republic
- ¹²⁹ State Research Center Institute for High Energy Physics (Protvino), NRC KI, Russia
- ¹³⁰ Particle Physics Department, Rutherford Appleton Laboratory, Didcot, United Kingdom
- ¹³¹ ^(a) INFN Sezione di Roma; ^(b) Dipartimento di Fisica, Sapienza Università di Roma, Roma, Italy
- ¹³² ^(a) INFN Sezione di Roma Tor Vergata; ^(b) Dipartimento di Fisica, Università di Roma Tor Vergata, Roma, Italy
- ¹³³ ^(a) INFN Sezione di Roma Tre; ^(b) Dipartimento di Matematica e Fisica, Università Roma Tre, Roma, Italy
- ¹³⁴ ^(a) Faculté des Sciences Ain Chock, Réseau Universitaire de Physique des Hautes Energies - Université Hassan II, Casablanca; ^(b) Centre National de l'Énergie des Sciences Techniques Nucleaires, Rabat; ^(c) Faculté des Sciences Semlalia, Université Cadi Ayyad, LPHEA-Marrakech; ^(d) Faculté des Sciences, Université Mohamed Premier and LPTPM, Oujda; ^(e) Faculté des sciences, Université Mohammed V, Rabat, Morocco
- ¹³⁵ DSM/IRFU (Institut de Recherches sur les Lois Fondamentales de l'Univers), CEA Saclay (Commissariat à l'Énergie Atomique et aux Énergies Alternatives), Gif-sur-Yvette, France
- ¹³⁶ Santa Cruz Institute for Particle Physics, University of California Santa Cruz, Santa Cruz CA, United States of America
- ¹³⁷ Department of Physics, University of Washington, Seattle WA, United States of America
- ¹³⁸ Department of Physics and Astronomy, University of Sheffield, Sheffield, United Kingdom
- ¹³⁹ Department of Physics, Shinshu University, Nagano, Japan
- ¹⁴⁰ Fachbereich Physik, Universität Siegen, Siegen, Germany

- ¹⁴¹ Department of Physics, Simon Fraser University, Burnaby BC, Canada
- ¹⁴² SLAC National Accelerator Laboratory, Stanford CA, United States of America
- ¹⁴³ ^(a) Faculty of Mathematics, Physics & Informatics, Comenius University, Bratislava; ^(b) Department of Subnuclear Physics, Institute of Experimental Physics of the Slovak Academy of Sciences, Kosice, Slovak Republic
- ¹⁴⁴ ^(a) Department of Physics, University of Cape Town, Cape Town; ^(b) Department of Physics, University of Johannesburg, Johannesburg; ^(c) School of Physics, University of the Witwatersrand, Johannesburg, South Africa
- ¹⁴⁵ ^(a) Department of Physics, Stockholm University; ^(b) The Oskar Klein Centre, Stockholm, Sweden
- ¹⁴⁶ Physics Department, Royal Institute of Technology, Stockholm, Sweden
- ¹⁴⁷ Departments of Physics & Astronomy and Chemistry, Stony Brook University, Stony Brook NY, United States of America
- ¹⁴⁸ Department of Physics and Astronomy, University of Sussex, Brighton, United Kingdom
- ¹⁴⁹ School of Physics, University of Sydney, Sydney, Australia
- ¹⁵⁰ Institute of Physics, Academia Sinica, Taipei, Taiwan
- ¹⁵¹ Department of Physics, Technion: Israel Institute of Technology, Haifa, Israel
- ¹⁵² Raymond and Beverly Sackler School of Physics and Astronomy, Tel Aviv University, Tel Aviv, Israel
- ¹⁵³ Department of Physics, Aristotle University of Thessaloniki, Thessaloniki, Greece
- ¹⁵⁴ International Center for Elementary Particle Physics and Department of Physics, The University of Tokyo, Tokyo, Japan
- ¹⁵⁵ Graduate School of Science and Technology, Tokyo Metropolitan University, Tokyo, Japan
- ¹⁵⁶ Department of Physics, Tokyo Institute of Technology, Tokyo, Japan
- ¹⁵⁷ Department of Physics, University of Toronto, Toronto ON, Canada
- ¹⁵⁸ ^(a) TRIUMF, Vancouver BC; ^(b) Department of Physics and Astronomy, York University, Toronto ON, Canada
- ¹⁵⁹ Faculty of Pure and Applied Sciences, and Center for Integrated Research in Fundamental Science and Engineering, University of Tsukuba, Tsukuba, Japan
- ¹⁶⁰ Department of Physics and Astronomy, Tufts University, Medford MA, United States of America
- ¹⁶¹ Centro de Investigaciones, Universidad Antonio Narino, Bogota, Colombia
- ¹⁶² Department of Physics and Astronomy, University of California Irvine, Irvine CA, United States of America
- ¹⁶³ ^(a) INFN Gruppo Collegato di Udine, Sezione di Trieste, Udine; ^(b) ICTP, Trieste; ^(c) Dipartimento di Chimica, Fisica e Ambiente, Università di Udine, Udine, Italy
- ¹⁶⁴ Department of Physics, University of Illinois, Urbana IL, United States of America
- ¹⁶⁵ Department of Physics and Astronomy, University of Uppsala, Uppsala, Sweden
- ¹⁶⁶ Instituto de Física Corpuscular (IFIC) and Departamento de Física Atómica, Molecular y Nuclear and Departamento de Ingeniería Electrónica and Instituto de Microelectrónica de Barcelona (IMB-CNM), University of Valencia and CSIC, Valencia, Spain
- ¹⁶⁷ Department of Physics, University of British Columbia, Vancouver BC, Canada
- ¹⁶⁸ Department of Physics and Astronomy, University of Victoria, Victoria BC, Canada
- ¹⁶⁹ Department of Physics, University of Warwick, Coventry, United Kingdom
- ¹⁷⁰ Waseda University, Tokyo, Japan
- ¹⁷¹ Department of Particle Physics, The Weizmann Institute of Science, Rehovot, Israel
- ¹⁷² Department of Physics, University of Wisconsin, Madison WI, United States of America
- ¹⁷³ Fakultät für Physik und Astronomie, Julius-Maximilians-Universität, Würzburg, Germany
- ¹⁷⁴ Fakultät für Mathematik und Naturwissenschaften, Fachgruppe Physik, Bergische Universität

Wuppertal, Wuppertal, Germany

¹⁷⁵ Department of Physics, Yale University, New Haven CT, United States of America

¹⁷⁶ Yerevan Physics Institute, Yerevan, Armenia

¹⁷⁷ Centre de Calcul de l'Institut National de Physique Nucléaire et de Physique des Particules (IN2P3), Villeurbanne, France

^a Also at Department of Physics, King's College London, London, United Kingdom

^b Also at Institute of Physics, Azerbaijan Academy of Sciences, Baku, Azerbaijan

^c Also at Novosibirsk State University, Novosibirsk, Russia

^d Also at TRIUMF, Vancouver BC, Canada

^e Also at Department of Physics & Astronomy, University of Louisville, Louisville, KY, United States of America

^f Also at Department of Physics, California State University, Fresno CA, United States of America

^g Also at Department of Physics, University of Fribourg, Fribourg, Switzerland

^h Also at Departament de Física de la Universitat Autònoma de Barcelona, Barcelona, Spain

ⁱ Also at Departamento de Física e Astronomia, Faculdade de Ciências, Universidade do Porto, Portugal

^j Also at Tomsk State University, Tomsk, Russia

^k Also at Università di Napoli Parthenope, Napoli, Italy

^l Also at Institute of Particle Physics (IPP), Canada

^m Also at Department of Physics, St. Petersburg State Polytechnical University, St. Petersburg, Russia

ⁿ Also at Department of Physics, The University of Michigan, Ann Arbor MI, United States of America

^o Also at Louisiana Tech University, Ruston LA, United States of America

^p Also at Institutio Catalana de Recerca i Estudis Avancats, ICREA, Barcelona, Spain

^q Also at Graduate School of Science, Osaka University, Osaka, Japan

^r Also at Department of Physics, National Tsing Hua University, Taiwan

^s Also at Department of Physics, The University of Texas at Austin, Austin TX, United States of America

^t Also at Institute of Theoretical Physics, Iliia State University, Tbilisi, Georgia

^u Also at CERN, Geneva, Switzerland

^v Also at Georgian Technical University (GTU), Tbilisi, Georgia

^w Also at Ochadai Academic Production, Ochanomizu University, Tokyo, Japan

^x Also at Manhattan College, New York NY, United States of America

^y Also at Hellenic Open University, Patras, Greece

^z Also at Institute of Physics, Academia Sinica, Taipei, Taiwan

^{aa} Also at Academia Sinica Grid Computing, Institute of Physics, Academia Sinica, Taipei, Taiwan

^{ab} Also at School of Physics, Shandong University, Shandong, China

^{ac} Also at Moscow Institute of Physics and Technology State University, Dolgoprudny, Russia

^{ad} Also at Section de Physique, Université de Genève, Geneva, Switzerland

^{ae} Also at International School for Advanced Studies (SISSA), Trieste, Italy

^{af} Also at Department of Physics and Astronomy, University of South Carolina, Columbia SC, United States of America

^{ag} Also at School of Physics and Engineering, Sun Yat-sen University, Guangzhou, China

^{ah} Also at Institute for Nuclear Research and Nuclear Energy (INRNE) of the Bulgarian Academy of Sciences, Sofia, Bulgaria

^{ai} Also at Faculty of Physics, M.V.Lomonosov Moscow State University, Moscow, Russia

^{aj} Also at National Research Nuclear University MEPhI, Moscow, Russia

^{ak} Also at Department of Physics, Stanford University, Stanford CA, United States of America

^{al} Also at Institute for Particle and Nuclear Physics, Wigner Research Centre for Physics, Budapest,

Hungary

am Also at Flensburg University of Applied Sciences, Flensburg, Germany

an Also at University of Malaya, Department of Physics, Kuala Lumpur, Malaysia

ao Also at CPPM, Aix-Marseille Université and CNRS/IN2P3, Marseille, France

* Deceased